Chloride Penetration Resistance and Link to Service Life Design of Virginia Bridge Decks

Elizabeth Rose Bales

Thesis submitted to the faculty of the Virginia Polytechnic Institute and State University in partial fulfillment of the requirements for the degree of

Master of Science
In
Civil Engineering

Madeleine M. Flint
Sean P. McGinnis
Carin L. Roberts-Wollmann

April 25, 2016
Blacksburg, Virginia

Keywords: bridge deck, chloride diffusion, corrosion, service life, life cycle cost

Chloride Penetration Resistance and Link to Service Life Design of Virginia Bridge Decks

Elizabeth Rose Bales

ABSTRACT

Reinforced concrete (RC) bridge decks are exposed to chlorides from deicing salts. Chloride ingress in RC initiates corrosion of the reinforcing steel. The high costs of corrosion have sparked interest in service life design of bridge decks. This thesis characterized the exposure conditions of Virginia, including temperature and surface chloride concentration, as well as Virginia concrete mix properties, including initial chloride concentration and chloride migration coefficient. The service life estimations for a case study bridge in Virginia from three service life models were compared. The first model is based on the *fib* Bulletin 34 Model Code for Service Life Design, the second is a finite element solution of the *fib* Bulletin, and the third accounts for a time-, temperature-, moisture-, and concentration-dependent apparent diffusion coefficient. A sensitivity analysis was completed on the three models showing that the most important variables in these models are the aging coefficient and surface chloride concentration. Corresponding life cycle cost analyses were completed for plain and corrosion resistant reinforcing steel. This thesis showed that the error function solution underestimates chloride ingress. The life cycle cost analysis of plain and corrosion resistant reinforcing steels show that overestimation of service life leads to underestimation of life cycle costs.

Chloride Penetration Resistance and Link to Service Life Design of Virginia Bridge Decks

Elizabeth Rose Bales

ABSTRACT (public)

Corrosion of reinforcement in reinforced concrete (RC) bridge decks causes serviceability issues and can lead to loss of strength. The annual costs associated with corrosion in bridges were estimated at $8.3 billion USD in 2002 (Koch et al. 2002). Engineers hope to design structures with longer service lives. The service life is the period during which a structure does not require any restoration or repairs to remain function, only routine maintenance operations. This work compares three service life estimating models for a bridge deck in Virginia. Life cycle cost (LCC) for different types of reinforcement for the bridge deck over its service life were also compared. LCC is an analysis method accounting for initial and recurring costs of a product over its lifetime. The LCC comparison showed that corrosion resistant reinforcing is more cost effective than plain reinforcing. Also, overestimating a bridge deck's service life can lead to underestimating the LCC of the reinforcement.

ACKNOWLEDGEMENTS

I must thank the Virginia Department of Transportation with the Strategic Highway Research Program 2 for funding my work in this project.

I would first like to thank Dr. Madeleine Flint, my advisor, for always answering my questions in ways that inspired more learning, and for sharing your knowledge with me. I am thankful for not only the development of my skills to finish this project, but also the interest in the subject. I am a better communicator and person after this experience.

I also thank my committee members, Dr. Carin Roberts-Wollmann, and Dr. Sean McGinnis, for reading through drafts, providing invaluable comments, and keeping my eyes open to the larger scope and impacts of this project. Michael Brown and Prasad Nallapaneni at VDOT also deserve a thank you for answering my many questions about Virginia bridges quickly and thoroughly.

I cannot leave out my friends here at Virginia Tech, who have celebrated successes with me and encouraged me during times when success seemed far-off. Shear Studs unite.

I would like to thank my parents for their unending love and support and for instilling in me a desire to learn and a passionate work ethic.

Finally, I must thank my husband, Dustin. I would not have completed this thesis if it weren't for you. You probably know more about chloride ingress than you ever wanted to, but for your support and love I am forever grateful. *Thank you*.

TABLE OF CONTENTS

LIST OF FIGURES

LIST OF TABLES

1. INTRODUCTION

Motivations

The average age of bridges in Virginia is 48 years, with 25% of bridges being older than 60 years (VDOT 2015). Many of these bridges were only designed to last 50 years before needing major repairs or even replacement. Costly repairs and maintenance are required to keep bridges functioning at a safe level as they age; the older the bridge, the greater the exposure to the elements. Bridge decks deteriorate from the traffic loads, but also from the damage that chloride-laden environments can cause. Deicing salts, seawater, even chlorides in the atmosphere contribute to corrosion of the reinforcing steel in bridge decks.

Corrosion from chloride ingress is not the only mechanism causing bridge deck deterioration, but as infrastructure continues to age, it becomes a larger problem because chloride ingress increases over time. The direct cost of corrosion for highway bridges nationwide was estimated at $8.3 billion annually in 2002 USD (Koch et al. 2002).

These cost and maintenance issues bring service life design to engineers' attention. A product's service life represents its expected lifetime requiring only routine maintenance operations; no major repairs are necessary during a service life. With upkeep costs for existing structures rising, service life goals for new designs are changing. At the federal level, the goal of designing a bridge deck with a service life of 100 years is being promoted. This work aims to investigate these topics for bridge deck designs in Virginia.

Problem Definition

Bridges constructed in Virginia before 2007 expect a service life of 50 years; bridges constructed since 2007 expect a service life of 75 years (VDOT 2015). These service lifetimes are a

byproduct of other design limit states; service life design was not explicitly completed. Since 2007, the Virginia Department of Transportation (VDOT) has implemented new concrete designs and reinforcing steel types in attempts to reach an even greater service life of 100 years. VDOT has not yet quantified the impact of the new technologies on service life. VDOT hopes to include 100-year service life as a new limit state in the design of new bridge decks in Virginia. It is important to analyze the new technologies for service life impacts to validate the new design technologies.

In this work, service life is defined as the time between the completion of construction of the bridge deck and the end of the corrosion initiation period. The service life period is the time during which the bridge deck should not need to undergo major structural repairs due to deterioration from chloride ingress. However, routine maintenance of the bridge deck is necessary during this time.

Once the design technologies affecting service life design are understood, the costs must be considered over the life of the structure. For a structure designed to last 100 years, more than just initial costs need to be considered. Life cycle costs consider the original construction costs and costs associated with maintenance schedules over the service life of a structure.

Aims and Objective

This thesis presents a parameter study for and comparison between service life design models for Virginia bridge deck designs. The aim of this work is to characterize Virginia exposure zones and concrete mix design parameters, compare service life models for a case study bridge, and complete preliminary life cycle cost studies. Characterizing Virginia's exposure zones will quantify the environmental effects different regions of Virginia impose on service life.

Comparing service life models reveals strengths and weaknesses of different service life predictors. Evaluating the service life of bridge decks in Virginia based on region-specific exposures and VDOT-specific design elements allows comparison of service life throughout Virginia. Life cycle cost analysis aims to quantify the costs associated with the bridge deck while considering its entire service life. This work aims to provide a basis of knowledge to allow VDOT to implement service life design for new bridge decks.

Overview of Methods

Historical temperature, snowfall, and precipitation data were analyzed to characterize exposure conditions in Virginia. Exposure conditions include surface chloride concentration and ambient air temperature. This work characterized surface chloride concentrations first through a compilation of historical test results. The *fib* Bulletin 34 Model Code for Service Life Design details durability models and frameworks for performance-based designs. The *fib* method for predicting surface chloride concentrations was also used. VDOT laboratories completed the characterization of Virginia concrete mix designs. VDOT laboratories characterized the concrete parameters: initial chloride concentration and the chloride migration coefficient.

Three different models in this work model chloride ingress and predict service life. All three models are based on Fickean diffusion, but with variations on the solution technique. The *fib* Bulletin 34 Model Code for Service Life Design provides the basis for the first model, Model fib. Research initiated by The Strategic Highway Research Program 2 (SHRP 2) for improving highway safety, reducing congestion, and improving methods for renewing bridges and roads has renewed interest in service life design. VDOT is part of the SHRP 2 program that suggests the implementation of *fib* Bulletin 34 Model Code for Service Life Design (fib 2006). The *fib* model

offers fully probabilistic methods for service life design that aim to balance accuracy and ease-of-use. Model fib-FEM is a finite element solution also based on the *fib* Model. The third model, Model TTMC-FEM is a finite element solution with a time-, temperature-, moisture-, and concentration-dependent diffusion coefficient. This work compares the service life predictions from all three models for a case study bridge in Virginia. Section 1.2 describes these models in more detail. A sensitivity analysis was completed on each service life model to identify the amount of influence of each variable on the models' results. A comparison of service life predictions from Model fib for the case study bridge existing in the different regions of Virginia was completed. The exposure conditions changed for each regional location while the remainder of the design variables remained constant.

For this case study bridge, a life cycle cost analysis was also completed. The life cycle costing compared the cost of plain reinforcing steel and corrosion resistant reinforcing steel over the predicted service life associated with each reinforcing steel type.

Overview

The remainder of this chapter introduces the motivations, objectives, and methods for the three major contributions of this work: Characterization, Model Comparison, and Life Cycle Cost Analysis.

The remainder of this thesis details further the methods, results, and conclusions of the studies introduced in this chapter. Chapter 2 Background details past research completed in this area and provides technical information on the topics covered. Chapter 3 Methods details the methods used in completing the contributions of this work. Chapter 4 Results details, interprets, and

discusses the results of the studies completed. Chapter 5 Conclusions summarizes the results, conclusions, and significance of this work. Suggestions for future work are also included.

1.1. Characterization

The first contribution of this work is the characterization of Virginia exposure conditions and concrete mix designs. Accurate service life predictions require accurate environmental conditions, and any variables need to be quantified to complete a service life design. These include surface chloride concentration, initial chloride concentration, diffusion coefficient, and regional temperature. Laboratory tests or historical test results often provide data to quantify these variables.

1.1.1. Exposure

The state of Virginia experiences a wide variety of temperatures and exposure conditions; the state was divided into six regions to provide a finer representation of the conditions a new bridge deck might experience.

This work quantified **regional temperatures** based on historical data for all models since the ambient air temperature is known to affect the diffusion coefficient. For Models fib and fib-FEM, an average yearly temperature was used; Model C uses a time-dependent temperature, so a sinusoidal regression of the temperature data was used.

Surface chloride concentrations from applications of deicing salts, seawater, or brackish water, must be known to predict service life. To evaluate surface chloride concentrations through field testing, sample cores of the deck are extracted, and the concentration of chlorides at the surface are recorded. Studies of the historical averages of surface chloride concentration due to deicing

environments in Virginia were aggregated. This historical data was used as the predicted surface chloride concentrations in the service life models: *predicted* because since the structure does not exist yet, its surface chloride concentration does not exist either. Using historical averages provides a reasonable representation of what the surface chloride concentration may be for a new structure. The *fib* Bulletin details a method for calculating surface chloride concentration based on precipitation and amounts of chloride used during deicing events. The resulting surface chloride concentrations from the *fib* method were compared to the historical data from testing.

1.1.2. Concrete Properties

VDOT has not traditionally characterized their concrete mixes used for bridge decks regarding service life design parameters. At the onset of this work, several bridge decks throughout Virginia, conforming to new service life oriented design specifications, were scheduled for concrete placement. Concrete samples from these castings were taken and used as the samples to be tested for the initial chloride concentration and chloride migration coefficient. VDOT laboratories completed the testing.

The **initial chloride concentration** is the chloride concentration that exists within the concrete at the onset of the service life due to aggregates, binders, or water used in the preparation of the mix. The initial chloride concentration is assumed to be uniform throughout the cross section of the deck. VDOT laboratories completed titration testing on concrete samples from the bridge deck samples to evaluate the initial chloride concentration of the concrete at the time of the placement.

The **chloride migration coefficient** is the penetration resistance of the concrete to chlorides. The chloride profiling method used on existing reinforced concrete (RC) structures or testing of

laboratory specimen can determine the chloride penetration resistance of the concrete. VDOT laboratories conducted NT Build 492 test on the bridge deck samples to determine the chloride migration coefficient. The NT Build 492 test is used to determine the chloride migration coefficient of a concrete sample through non-steady-state-migration experiments (NordTest 1999)

1.2. Model Comparison

The second contribution of this work is the evaluation of three service life models and a comparison of the results between them. This section introduces the models used to predict the service life and estimate the probability of corrosion initiation of a bridge deck within 100 years in due to chloride ingress of a case study bridge. All models require knowledge of material parameters and exposure conditions relating to local methods and environmental conditions.

1.2.1. Model fib

The fully probabilistic equation that the *fib* model uses for chloride ingress is

$$C(x = a, t) = C_0 + \left(C_{s,\Delta x} - C_0\right)\left[1 - erf\frac{a - \Delta x}{2\sqrt{D_{app,C}t}}\right] \qquad \text{Equation 1}$$

where $C(x = a, t)$ is the chloride concentration at depth x equal to a and time, t, C_0 is the initial chloride concentration, $C_{s,\Delta x}$ is the surface chloride concentration, a is the distance to the reinforcement, Δx is the depth of the convection zone, and $D_{app,C}$ is the apparent chloride diffusion coefficient. The chloride concentration $C_{(x=a,t)}$ at the depth of the reinforcing steel can then be compared to the critical chloride threshold, C_{crit}.

1.2.2. Model fib-FEM

The first finite element model used in this work herein is also based on the *fib* Bulletin methodology. Model fib-FEM solves Fickian diffusion using the finite element method using the *fib* Bulletin definition of variables.

1.2.3. Model TTMC-FEM

The third model, Model TTMC-FEM, is a finite element model that includes a time-, moisture-, temperature-, and concentration- (TTMC) dependent apparent diffusion coefficient. Model TTMC-FEM illustrates differences between constant boundary conditions, as in Model fib and Model fib-FEM, and non-constant boundary conditions.

1.2.4. Case Study Bridge

Service life analysis was completed on a case study bridge deck in Virginia using the three models. This work compared service life distributions and the probability of failure from the three models.

The case study bridge was also modeled as if it were located in each of the six regions in Virginia to show the impact that regional exposure zones have on service life.

1.2.5. Monte Carlo Simulation

While probabilistic models are often preferred because they better represent the stochastic nature of variables, a probabilistic design requires more data and a deeper understanding of the distribution types of the variables. This work used probabilistic design because of its increased accuracy in representation of variables.

The stochastic nature of the variables and nonlinear limit state was accounted for using Monte Carlo simulations. Each simulation randomly samples from a variables' distribution. After a specific number of simulations, the numerical solution is converged. For each Model (fib, fib-FEM, and TTMC-FEM) in this work, Monte Carlo simulations were completed to converge on the service life distribution and the probability of corrosion initiation.

1.2.6. Sensitivity Analysis

A sensitivity analysis was also completed on all three models to quantify variable uncertainty. Since all models have some uncertainty associated with the variables (either distribution type, means, or variances), a sensitivity analysis was completed to evaluate the importance of each variable concerning the probability of failure. Because many input variables are uncertain, it is important to identify which variables most influence the outcome of each model; the focus can then be placed on deepening understanding the most influential variables.

1.3. Life Cycle Cost Analysis

The final contribution of this work is to complete a life cycle cost (LCC) analysis of alternatives reinforcement types for bridge decks in Virginia. Service life design models can be to optimize service life and LCC. The service life design coordinated with an LCC can inform to the most optimal design regarding service life and cost over the life of the bridge.

An estimated uniform annual cost (EUAC) calculates the cost of a product considering its entire service life. EUAC was used in this work to compare the costs of plain reinforcing steel and corrosion resistant reinforcing steel for the duration of their respective predicted service life.

2. BACKGROUND

Chloride penetration initiates service life failures in reinforced concrete (RC) bridge decks because of corrosion of the reinforcing steel. Because of the high costs associated with corrosion, service life design has become more prevalent. Service life design in Virginia has not been utilized as a regular part of the design process to date. The Virginia Department of Transportation (VDOT) has implemented the use of low-cracking concrete mix designs and corrosion-resistant reinforcing steel but has not quantified the effects these new technologies have on a bridge deck's service life.

Service life design considers very specific design elements and exposure conditions. For this reason, before service life designs can be completed on bridge decks in Virginia, Virginia-specific variables must be quantified. The service life design models in this work are compared to other models and validated against a chloride profile from an existing bridge deck. The comparison and validation allow differences, advantages, and disadvantages of models to be evaluated.

This chapter provides technical background and, when applicable, an overview of previous research on Exposure Characterization,

Mix Design Characterization, Physics of RC Corrosion and Deterioration, Mathematical Models for Chloride Ingress, Probabilistic Modeling, and Life Cycle Cost.

2.1. Exposure Characterization

2.1.1. Regional Temperatures

Several different climate zones exist in Virginia (NOAA). These regions not only experience varied temperatures but weather conditions as well. While the geographic separation of these regions has been established, it has not been explored what effect different exposures in each region of Virginia have on service life design.

2.1.2. Surface Chloride Concentration in Virginia

Surface chloride concentration of an RC structure is a function of that structures' exposure and cement composition. A number of studies have characterized chloride exposure in the state of Virginia. It has been verified that the convection zone depth (depth at which the surface chloride concentration stabilizes) is approximately 12.7 mm because of the chlorides being washed out of the concrete just below the deck surface (Cady and Weyers 1983). Tang showed that surface chloride concentrations on bridges vary with time (1996). Williamson modeled surface chloride concentrations of Virginia bridge decks as constant and non-constant and found that the service life predictions varied by up to 15% (2007). This thesis used a surface chloride concentration that is not time dependent and is based on previous test results on Virginia bridge decks. Investigations into surface chloride concentrations of Virginia bridges have also been completed by (Kirkpatrick 2001; Williamson 2007).

The *fib* Bulletin provides methodologies for calculating the surface chloride concentration based on precipitation and deicing salt application. To date, this methodology has not been tested or validated in Virginia.

2.2. Mix Design Characterization

For service life modeling of bridges in Virginia, it is necessary to be able to quantify the input variables for the models. The initial chloride concentration and diffusion coefficient are variables

that are dependent on the concrete mix design used. The Virginia Department of Transportation specifies the concrete to be used on a bridge deck with a performance specification. This leaves the design of the concrete mix to be completed (within the specification limits) to the concrete supplier, which can lead to concrete with variable properties.

2.2.1. Initial Chloride Concentration

Initial chlorides describe chlorides that exist within the concrete since it was originally mixed; they can come from chlorides in the aggregate or the water used in the concrete mix. The initial chloride concentration of Virginia bridge decks has been quantified in a past test program (Williamson 2007). The concrete mixes VDOT presently uses differ from those tested by Williamson, so additional initial chloride concentration testing took place for this work.

2.2.2. Chloride Penetration Resistance

The chloride penetration resistance of Virginia bridge decks has been found through chloride profiling of existing bridges (Williamson 2007). The chloride penetration resistance of VDOT's current standard for bridge deck concrete has not been previously tested. It is advantageous to test the concrete mix for its chloride penetration resistance during construction as the concrete properties at this point are well documented. These properties can get lost over the years, making testing 20 years later less insightful.

Several laboratory tests can be conducted to calculate the chloride penetration resistance of concrete. The NT Build 492 (NordTest) is common in Europe. The competing standard in the US is ASTM C1202. Bagheri and Zangeneh verified that the ASTM C1202 method underestimates chloride resistance due to temperature effects (2012). For this reason, and to increase familiarity in the United States with the NordTest, it was used in this work. The NordTest is a non-steady-

state migration test that allows for the determination of the chloride migration coefficient. This test measures the resistance of concrete to chloride penetration based on the depth of penetration from testing (NordTest 1999).

2.3. Physics of RC Corrosion and Deterioration

In service life prediction of reinforced concrete (RC) structures, chloride ingress is often the only deterioration mechanism considered. Chloride ingress can lead to corrosion of the reinforcing steel. This section details the physics associated with chloride ingress and corrosion.

2.3.1. Chloride Ingress

Applied chlorides penetrate the concrete surface, and travel through concrete pore spaces (Poulsen and Mejlbro 2010). The method of travel of the chlorides can be diffusion, permeation, convection, and migration. Diffusion occurs when chlorides travel from an area of higher concentration (e.g. seawater) to an area of lower concentration (e.g. the concrete pore space). Convection takes place in cases where the movement of moisture carries chlorides. Permeation occurs when chlorides are driven into the concrete because of a difference in hydraulic pressure. Migration occurs because of a difference in electric potential. Diffusion is the primary method of transport in saturated conditions (Stanish et al. 2001). Bridge decks are not considered saturated, as they experience wet-dry cycles. However, an ‘apparent’ diffusion method is used to model chloride ingress in bridge decks, as explained in Section 2.4, Mathematical Models for Chloride Ingress.

Once chlorides have penetrated the RC surface, they can exist in two states: bound and free. Free chlorides exist dissolved in the pore solution, free to travel through the pores. Bound chlorides

are bound to the surfaces of or incorporated into cement hydration products (Martın-Pérez et al. 2000). This work reports the total chloride concentrations, bound and free, as a mass percentage of the binder materials (i.e., cement and supplementary cementitious materials) in the concrete.

2.3.2. Corrosion of Steel

Chloride ingress in plain, unreinforced concrete does not initiate any degradation of the concrete, but chloride ingression is troublesome when the concrete is reinforced with steel. The corrosion of reinforcing steel leads to degradation of the surrounding concrete. When steel is placed in concrete, a passive layer of corrosive products develops around the reinforcement because of the pH level of concrete. This passive layer protects the steel from corrosion. However, once the chloride levels at the reinforcing steel reach a critical concentration, they will begin the active corrosion initiation phase, corroding the passive, protective layer around the steel. This critical concentration of chlorides depends on the reinforcing steel; corrosion resistant steels have a higher critical threshold for chloride levels than traditional, plain reinforcing steel (Hurley and Scully 2006). The corrosive products affect the durability of the surrounding concrete through cracking, loss of bond between the reinforcing steel and concrete, loss of steel area, and spalling. The occurrence of these issues can lead to serviceability issues as well as loss of strength.

2.4. Mathematical Models for Chloride Ingress

This section details the mathematics used to model diffusion and previous research completed on this topic.

One-dimensional diffusion in concrete can be represented by Fick's second law of diffusion, shown below in Equation 2. While a one-dimensional equation neglects edge effects, the

diffusion of chlorides in RC bridge decks is primarily a one-dimensional process. This law states that the change in chloride concentration per unit time is equal to the gradient of concentration per unit length.

$$\frac{\partial C}{\partial t} = \frac{\partial}{\partial x}\left\{D\frac{\partial C}{\partial x}\right\} \qquad \text{Equation 2}$$

where C is the concentration of an ionic species, D is the proportionality constant, t is time, and x is the depth from the exposed surface. In the case of chloride ingress, D represents the chloride diffusion coefficient.

Because Fick's law only represents the mathematics associated with diffusion, an apparent diffusion coefficient can be used to account for other methods of transportation (migration, permeation, and convection) and other effects that cause the diffusion coefficient to be non-constant. For example, the diffusion coefficient is known to decrease as the concrete cures (Andrade et al. 2011) because the resistance to chloride ingress increases as the pore structure changes with the hydration of the cement; this is known as aging effects or maturation. The maturation function is often 'fit' to data of apparent diffusion coefficients versus age for curing ages up to 56 or 90 days. The maturation function is discussed in further detail in Section 3.3.1, Model fib.

The chloride ingress models used in this work fall into two categories: error function solution or finite element solution. Error function solutions allow for an approximate solution to Fickian diffusion. Finite element solutions allow for non-constant boundary conditions while solving Fickian diffusion.

2.4.1. Error Function

The error function is an approximate analytical solution that closely matches the solution to Fick's law. The chloride at a specific depth and time can be found by

$$C_{(x,t)} = C_0\left(1 - \text{erf}\left(\frac{x}{2\sqrt{D_c t}}\right)\right) \quad \text{Equation 3}$$

where $C_{(x,t)}$ is the chloride concentration at depth, x, and time, t, C_0 is the surface chloride concentration and D_c is the diffusion coefficient. Use of the error function (abbreviated erf) solution provides a discrete solution, meaning that the chloride concentration at any depth and time are independent of the chloride concentration at any other point in time. Several different applications of the error function solution have been completed.

The *fib* Bulletin 34 Model Code for Service Life Design details a methodology for completing service life predictions using

$$C(x = a, t) = C_0 + \left(C_{s,\Delta x} - C_0\right)\left[1 - erf\frac{a - \Delta x}{2\sqrt{D_{app,C}t}}\right] \quad \text{Equation 4}$$

where $C(x = a, t)$ is the chloride concentration at depth, x, and time of expected service life, t, C_0 is the initial chloride concentration, $C_{s,\Delta x}$ is the surface chloride concentration, Δx is the depth of the convection zone, a is the depth of the reinforcing steel, and $D_{app,C}$ is the apparent diffusion coefficient. $D_{app,C}$ for new structures is based on chloride migration test results (NordTest). The apparent diffusion coefficient in the *fib* Bulletin accounts for temperature effects and age effects. It is also calibrated against chloride profiles from chloride profiling test results (fib 2006). This parameter is further discussed in Section 3.3.1, Model fib.

Mangat and Molloy presented an error function solution that accounts for the time dependent nature of the apparent diffusion coefficient based on the diffusion coefficient at reference time equal to one second (Mangat and Molloy 1994). Bamforth presented a similar model, accounting for the time dependence of diffusion, but the diffusion was based on the diffusion coefficient at reference time equal to one year (1999).

Because the Strategic Highway Research Program hopes to implement the use of the *fib* model code in states including Virginia, the *fib* model will be used in this work, and referred to as Model fib.

2.4.2. Finite Element

Tang and Gulikers showed that error function solutions can underestimate service life (2007). For this reason, this thesis compared an error function solution to two finite element solutions. The finite element solutions allow for time-dependent diffusion coefficient, as well as non-constant boundary conditions. The flexibility and more realistic modeling capability offered by these more complex finite element solutions was explored in this thesis.

The model titled Model fib-FEM in this work, is the finite element solution of Equation 1, using the *fib* Bulletin 34 (fib 2006) definition of variables. This comparison is the first for Virginia bridge deck service life design.

Saetta et al. developed a numerical procedure to describe the movement of chlorides in unsaturated and saturated concrete (1993). This model uses an apparent diffusion coefficient considering effects from temperature, age, and humidity. Saetta et al.'s model also considered time-dependent temperature and humidity. Some literature details methods using methods other

than apparent diffusion to capture more accurately the transportation methods other than diffusion. Nokken et al. developed a chloride ingress model that accounts for

- initial chloride,
- initial diffusion,
- time-dependence of diffusion,
- nonlinear binding,
- hydraulic pressure,
- time variant surface chloride concentration,
- monthly-variant temperature, and
- chloride build up due to wicking (2006).

Martın-Pérez et al. developed a finite element solution that coupled chloride transport, moisture diffusion, heat transfer, and oxygen transport (2001). Bastidas-Arteaga et al. model the coupled interactions of chloride transport, moisture transport, and heat transfer (Bastidas-Arteaga et al. 2011). Bastidas-Arteaga et al.'s model builds on Saetta et al.'s with the addition of accounting for binding capacity, time-dependent surface chloride concentration, and two-dimensional chloride ingress. There are also other complex and more computationally intense models that are not discussed here.

The second finite element model and third model used in this work is Model TTMC-FEM. Model TTMC-FEM solved Equation 2 using the finite element method. Model TTMC-FEM uses an apparent diffusion coefficient based on a combination of factors accounting for time-, temperature-, moisture-, and chloride concentration-dependence (Bastidas-Arteaga et al. 2011; Flint 2014). This model was the most complex in this thesis and chosen to evaluate the differences between *fib* based models and those accounting for moisture transport and binding.

2.5. Probabilistic Modeling

The stochastic nature of the variables in this work necessities a probabilistic modeling approach. Two methods are predominant in past research. Bastidas et al. used Monte Carlo simulation for the probabilistic solution of their corrosion initiation model due to the complexity of the limit state equations (2011). Williamson also used Monte Carlo simulation for service life prediction of Virginia bridges (2007). Saassouh and Lounis used first and second order reliability methods probabilistically model chloride induced corrosion (2012). First order reliability methods were found to be more efficient than Monte Carlo simulation (Saassouh and Lounis 2012). Because of the probabilistic nature of the variables, and nonlinear limit state, Monte Carlo simulation was used in this work.

2.5.1. Sensitivity Analysis

Literature in the area of sensitivity analysis on the chloride-induced corrosion models is less extensive than for chloride ingress models. Saassouh and Lounis performed sensitivity analysis on an error function solution using first and second order reliability methods (Saassouh and Lounis 2012), finding the cover depth to be the most important parameter. (Boddy et al. 1999) in developing a finite element chloride ingress model, also reported on the sensitivity study found that the service life prediction was most sensitive to the parameter that controls the rate of reduction of diffusivity, e.g. the aging coefficient. The sensitivity analysis completed in Boddy et al. used the one-factor-at-a-time method (1999). This consists of varying one input parameter while keeping all others at their base case.

Sensitivity analysis in this work was completed using a variation of the one-factor-at-a-time method, as the use of Monte Carlo Simulation precludes direct incorporation of reliability-based methods.

2.6. Life Cycle Cost

Bridge design must balance performance and cost. So, to consider the costs associated, life cycle cost (LCC) analyses can be used. LCC is a way to compare costs of design alternatives based on a specified time period; it is based on sophisticated methods that can be used to "demonstrate a transportation agency's commitment to infrastructure preservation" (FWHA 2015)

Williamson performed LCC analysis for Virginia bridge decks (2007). However, Williamson's work was based on service life models that predicted the life of the structure to exceed 100 years no matter what type of reinforcing steel was used; reinforcing steel choice was based on initial costs only. For this reason, reinforcing steel type did not influence the results of the LCC. Williamson found that one single maintenance strategy was not always best, but that the most appropriate maintenance strategy varied based on individual structure parameters. A method for calculating the annual equivalent of the life-cycle cost of bridges was proposed by (Stewart 2001). Where the annual equivalent cost scales a product's initial cost over its lifetime, accounting for interest.

LCC of bridge decks in the context of this work will compare the initial costs associated with plain and corrosion resistant reinforcing steel (MMFX) scaled to their respective predicted service lifetimes using the equivalent uniform annual cost (EUAC). More information about MMFX is given in Section 3.3.7 Model Comparison.

3. METHODS

This chapter details the methods completed in this thesis. A description of the work completed in the following areas is discussed: Exposure Characterization, Concrete Characterization, Service Life Models, and Life Cycle Cost.

3.1. Exposure Characterization

The division of Virginia into six climate regions was used, as shown in Figure 1. This separation is supported by and used in the work of (Williamson 2007). The exposure elements to be classified in this work included regional temperature and surface chloride concentration for the six climate and exposure regions of Virginia: Tidewater, Eastern Piedmont, Western Piedmont, Northern, Central Mountain, and Southwestern Mountain.

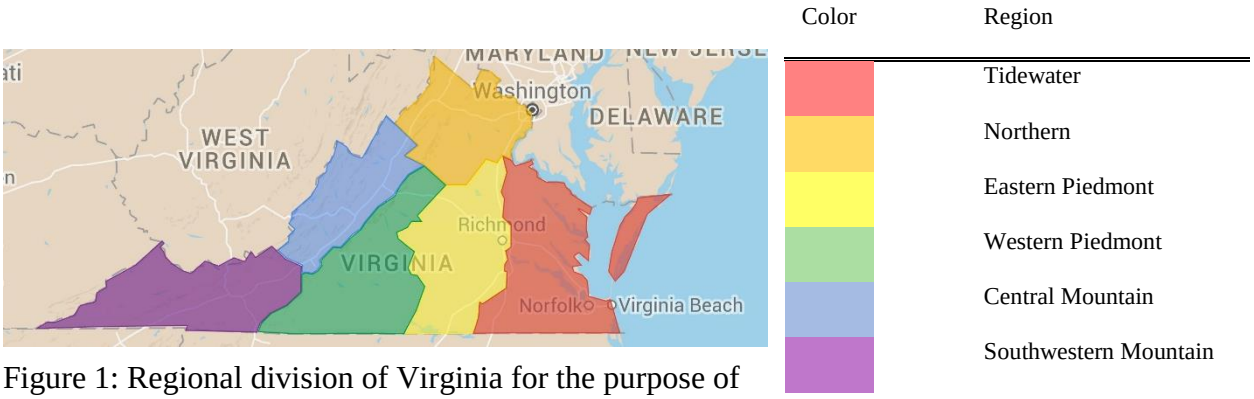

Figure 1: Regional division of Virginia for the purpose of exposure characterization

3.1.1. Temperature

The temperature was quantified as a yearly average and standard deviation, and also as a sinusoidal function of time over a year. The National Climate Data Center (NCDC) maintains historical weather and climate data and served as the source for the temperature data. Weather stations in each region were accessed to gather temperature data for the past 30 years; mean

monthly temperature data was recorded from July 1985 to June 2015. Table 26 in Appendix A lists the weather stations in Virginia used for temperature characterization. This provided 12 average monthly temperatures and yearly average and standard deviation temperatures in each region. For each of the six sets (one set for each region) of 12 monthly temperatures, sinusoidal regression equations were used to fit the data. The base equation that all region sets were fit to is given by Equation 5.

$$T = \text{a}\sin(\frac{2\pi}{12}t + c)+\text{d} \qquad \text{Equation 5}$$

where *T* is the temperature in Kelvin; *t* is the time in months; and *a*, *c*, and *d* are values set for each regional fit based on its regression. The MATLAB Curve Fitting tool was used to complete the regression analysis.

3.1.2. Surface Chloride Concentration

The surface chloride concentration of bridge deck is a function of its exposure; for this reason, surface chloride concentrations were studied by region in Virginia. Two methods were used to find surface chloride concentrations for the six Virginia climate regions. The first method was a collection of historical surface chloride concentration test results. The second method follows the *fib* method for calculating a surface chloride concentration based on the precipitation and chloride on the surface due to de-icing salts.

Historical Test Data Collection

Several investigations studied the surface chloride concentration of bridges in the state of Virginia (Kirkpatrick 2001; Williamson 2007). Their findings were compiled to establish the mean surface chloride concentration of bridges within the six climate regions of Virginia. The location of the bridges where surface chloride concentrations were reported is shown in Figure 2.

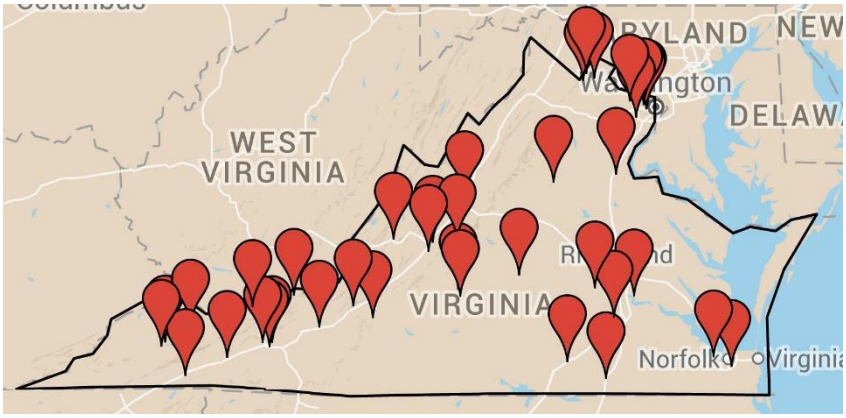

Figure 2: Location of bridges for which surface chloride concentration data was processed

The reported surface chloride concentrations for existing bridges were provided in units of weight of chlorides per volume of concrete.

Fib comparison

The *fib* Bulletin 34 details a method for calculating $C_{s\Delta x}$, a representative surface chloride concentration for a structure subject to deicing salts in the case that test data is not available (fib 2006). This method was compared to the results from the previous section to evaluate the *fib* method. This method is applicable in this work since the major source of chlorides in Virginia is from deicing salts.

Chloride contaminated water

According to the *fib* Bulletin, the concentration of chloride contaminated water due to deicing salts in is found by

$$C_{oR} = \frac{nc_{s,i}}{h_{s,i}} \qquad \text{Equation 6}$$

where C_{oR} is the average chloride concentration, n is the average number of salting events per year, $c_{s,i}$is the average amount of chloride spread per event, and $h_{s,i}$ is the amount of water from rain and snow during the events (fib 2006).

Chloride spread per event

The average amount of chloride spread was quantified by (Williamson 2007) for winter seasons in 2000-2001, 2001-2002, and 2002-2003 these are shown below in Table 1.

Table 1: Chloride exposure by region

Region	Chlorides, $\frac{lb\ Cl^-}{lane\ mile}$
Tidewater	798
Eastern Piedmont	1880
Western Piedmont	781
Northern	15501
Central Mountain	2381
Southwestern Mountain	2441

During these seasons, snowfall was observed as early as October and as late as April, therefore, the winter season herein is defined as October through April.

The chloride spread per event must be in units of $\frac{g}{m^2}$ for use in the *fib* method. To convert the amounts from $\frac{lb\ Cl^-}{lane\ mile}$ to be used in Equation 6, it was assumed that bridges in Virginia, on average, have a lane width of 12ft per lane. The amount of chloride per lane mile in Table 1 is represents the amount used in one winter season. One winter season was considered in this work because this method is not trivial, and a large amount of information must be gathered.

Number of salting events

To evaluate the number of salting events, daily snowfall, daily precipitation, and average daily temperature records from the NCDC was accessed. A list of weather stations utilized can be seen in Table 27 in Appendix A. These weather stations were accessed for October 1, 2000 through April 30, 2001. These dates were chosen since they corresponded with a winter season for which data on chloride spread per event data was available. A salting event was defined as a day where snowfall was greater than 0.00in and the daily temperature was between 20°F and 32°F. It is VDOT procedure to apply deicing salts only when the temperature is above 20°F because of their ineffectiveness when the temperature is less than 20°F (Williamson et al. 2007). The upper limit of 32°F was established because of the freezing point of water. Based on this qualifier, salting events were counted for each region in each of the three winter seasons.

Amount of precipitation from each event

Equivalent precipitation from snowfall and precipitation amounts recorded during the salting events were summed for the winter season. This value was used for $h_{s,i}$, precipitation from rain and snow. To quantify the amount of precipitation occurring with each salting event, precipitation accumulated during salting events was quantified. Since snowfall data is collected as a depth of snowfall, it must be converted to an equivalent rainfall amount to be used in Equation 6. The conversion between snowfall and equivalent precipitation, often called snow to liquid ratio, is a complicated one that depends on the ambient temperature during the snow fall event, and the snow density and molecular structure (Baxter et al. 2005). It is widely accepted that the snow to liquid ratio can be accurately calculated based on the air temperature alone (Kyle and Wesley 1997). (Kyle and Wesley 1997) details the snow to liquid ratio based on the

air temperature used in this work. These conversions were applied to the snowfall data to estimate an equivalent amount of precipitation occurring from the depth of snowfall.

Surface chlorides based on chloride contaminated water

fib instructs that once the chloride adsorption isotherm for the type of cement and the concrete composition are known, the chloride saturation content, or total chloride content, in the concrete at the surface, can be calculated from C_{oR}. The methods expressed in (Tang 1996) are to be carried out to calculate the chloride saturation content, $C_{S,0}$, where $C_{S,0}$ is equal to the surface chloride concentration at the depth of the convection zone, $C_{S,\Delta x}$. Tang (1996), however, does not detail a repeatable methodology converting a chloride solution on the concrete to a surface chloride concentration in the concrete. (Tang 1996) completed an experimental study on the chloride penetration, so a methodology may be inferred from the results, but *fib* is not clear as to how the calculation between C_{oR} and $C_{S,0}$ is to be completed. For this reason, the example given in *fib* was followed to find the surface chloride concentration, $C_{S,\Delta x}$. The binder content was assumed to 300 $\frac{kg}{m^3}$, and the water to cement ratio was assumed to be 0.50. From there, $C_{S,\Delta x}$ was determined based on the correlation provided between $C_{S,0}$ and $C_{S,\Delta x}$.

3.2. Concrete Characterization

The testing done to quantify the concrete mix characteristics, initial chloride concentration and the diffusion coefficient, was carried out by the laboratories of the Virginia Department of Transportation (VDOT). This section will detail the methods VDOT used to complete the tests.

VDOT specifies a performance-based concrete mix design for bridge deck design. So, for this testing program, one case study bridge was used as the source for concrete samples to be tested.

3.2.1. Initial chloride concentration

Chloride titrations were completed by VDOT to test for the initial, or background, chloride concentrations. The chloride titration test yields the total, bound and free, chlorides in the concrete sample. Initial chloride concentration tests were completed on concrete samples from four separate bridge decks in Virginia.

3.2.2. Chloride Migration Coefficient

To test for the chloride migration coefficient of the bridge deck concrete, the samples underwent NT Build 492 (NordTest) test at VDOT laboratories.

3.3. Service Life Models

This section describes the methods involved in the three service life models used in this work: Model fib, Model fib-FEM, Model TTMC-FEM.

3.3.1. Model fib

Model fib uses the *fib* Bulletin methodology for a fully probabilistic service life design (fib 2006) where the chloride concertation at a depth, x, and time, t, is found by

$$C(x = a, t) = C_0 + \left(C_{s,\Delta x} - C_0\right)\left[1 - erf\frac{a - \Delta x}{2\sqrt{D_{app,C}t}}\right] \quad \text{Equation 7}$$

where C_0 is the initial chloride concentration, $C_{s,\Delta x}$ is the surface chloride concentration at depth, Δx (which is the depth of the transfer function), erf represents the error function, a is the depth of the reinforcing steel, and $D_{app,C}$ is the apparent diffusion coefficient. The apparent diffusion coefficient, $D_{app,C}$ is given by

$$D_{app,C} = k_e \, D_{RCM,0} \, k_t \, A(t) \qquad \text{Equation 8}$$

where k_e is the environmental transfer parameter given by $D_{RCM,0}$ is the chloride migration coefficient, k_t is the transfer parameter, and $A(t)$ is the aging subfunction. The environmental transfer parameter, k_e is given by

$$k_e = \exp\left(b_e\left(\frac{1}{T_{ref}} - \frac{1}{T_{real}}\right)\right) \qquad \text{Equation 9}$$

where b_e is a regression variable, T_{ref} is the standard test temperature, T_{real} is the temperature of the structural element or the ambient air. $A(t)$, the aging subfunction is given by

$$A(t) = \left(\frac{t_0}{t}\right)^a \qquad \text{Equation 10}$$

where a is the aging exponent, t_0 is the reference point of time, and t is the intended service life time. The aging subfunction used here is based on a regression completed on hundreds of published chloride profiles from existing RC structures (fib 2006)

Failure is defined as $C(x = a, t) > C_{crit}$, where C_{crit} is the total chloride content that leads to depassivation of the reinforcing steel (fib 2006).

3.3.2. Model fib-FEM

Model fib-FEM is based on the *fib* Bulletin definition of variables (given in Section 3.3.1, but uses a finite element solution for Equation 11, as opposed to the *fib* error function solution.

$$\frac{\partial C}{\partial t} = \frac{\partial}{\partial x}\left\{D_{app,C}\frac{\partial C}{\partial x}\right\} \qquad \text{Equation 11}$$

In Equation 11, C represents the chloride concentration, x is the depth, and t is time. $D_{app,C}$ is the apparent diffusion coefficient with the same definition as in the *fib* Bulletin and can be found

using Equation 8-Equation 10. The differential equation was solved using the MATLAB 'pdepe' function with the initial condition as the initial chloride content C_0. The initial chloride content was assumed to be constant throughout the depth. The boundary conditions were as follows: at the 'surface' (taken as the depth of the convection zone, Δx) the concentration of chlorides was equal to the surface chloride concentration, $C_{s,\Delta x}$ and a no flux condition was prescribed at boundary farthest away from the exposed surface.

3.3.3. Model TTMC-FEM

Model TTMC-FEM, like Model fib-FEM, uses a finite element solution. However, Model TTMC-FEM does not use all the *fib* Bulletin definition of variables. Model TTMC-FEM solves the partial differential equation

$$\frac{\partial C}{\partial t} = \frac{\partial}{\partial x}\left\{D\frac{\partial C}{\partial x}\right\} \qquad \text{Equation 12}$$

where C is the chloride concentration, t is the time, x is the depth, and D is the apparent diffusion coefficient.

The apparent diffusion coefficient is found by

$$D = D_0\, f_T\, f_\varphi\, f_{bind}\, f_{age} \qquad \text{Equation 13}$$

where D_0 is the reference apparent diffusion coefficient, from chloride migration tests. The factors, f_T, f_φ, f_{bind}, and f_{age} are found by Equation 14 - Equation 19.

The temperature adjustment factor is found by

$$f_T = exp\left(b_e\left(\frac{1}{T_{ref}} - \frac{1}{T}\right)\right) \qquad \text{Equation 14}$$

where b_e is a regression variable as defined by (fib 2006), T_{ref} is the reference temperature. This equation for temperature effects is based on the Arrhenius function and is used in the *fib* Model for Service Life Design (fib 2006). It is also used in chloride ingress models completed by (Bastidas-Arteaga et al. 2011; Flint 2014) to account for temperature effects. T is the ambient air temperature, which estimated according to:

$$T(t) = a \sin\left(\frac{2\pi}{12}t + c\right) + d \qquad \text{Equation 15}$$

where t is the time in months; values a, c, and d are results from each regional nonlinear temperature regression.

The moisture adjustment factor is found by

$$f_\varphi = \left(1 + \frac{(1-\varphi)^4}{(1-\varphi_c)^4}\right)^{-1} \qquad \text{Equation 16}$$

where φ_c is the humidity at which the chloride diffusion coefficient drops halfway between its minimum and maximum; (Bažant and Najjar 1971) showed that this occurs when the humidity is equal to 0.75 for many different types of concrete. $\varphi(t)$ is the relative humidity in the concrete as a function of time and is found by

$$\varphi(t) = \frac{\varphi_{max} + \varphi_{min}}{2} + \frac{\varphi_{max} - \varphi_{min}}{2}\sin\big(2\pi(t)\big) \qquad \text{Equation 17}$$

where φ_{max} is the maximum humidity, φ_{min} is the minimum humidity, t is the time in years (Bastidas-Arteaga et al. 2011). This equation captures the sinusoidal trends of the humidity throughout the year.

The binding adjustment factor is found by a version of the Langmuir binding isotherm:

$$f_{bind} = \frac{1}{1 + \frac{\alpha_{bind}}{1(1 + \beta_{bindc_{Cl}})^2}}$$ Equation 18

where α_{bind} and $\beta_{bindc_{Cl}}$ are non-physical binding parameters (Flint 2014) used to account for the effects of chloride binding on the diffusion process. The binding parameters used for the Langmuir binding isotherm in this thesis were based on the test results of (Deng et al. 2013).

The aging adjustment factor is found by

$$f_{age} = \left(\frac{t_0}{t}\right)^{\alpha}$$ Equation 19

where t_0 is the reference time, t is the age of the bridge deck, and α is the aging coefficient as defined by (fib 2006). Model TTMC-FEM was solved using MATLAB's 'pdepe' function. The boundary conditions are as follows: at the 'surface' (taken as the depth of the convection zone, Δx) the concentration of chlorides is equal to the surface chloride concentration, $C_{s,\Delta x}$ and a no flux condition prescribed at boundary farthest away from the exposed surface.

Figure 3 shows the three service life models and illustrates graphically the differences in the solution techniques.

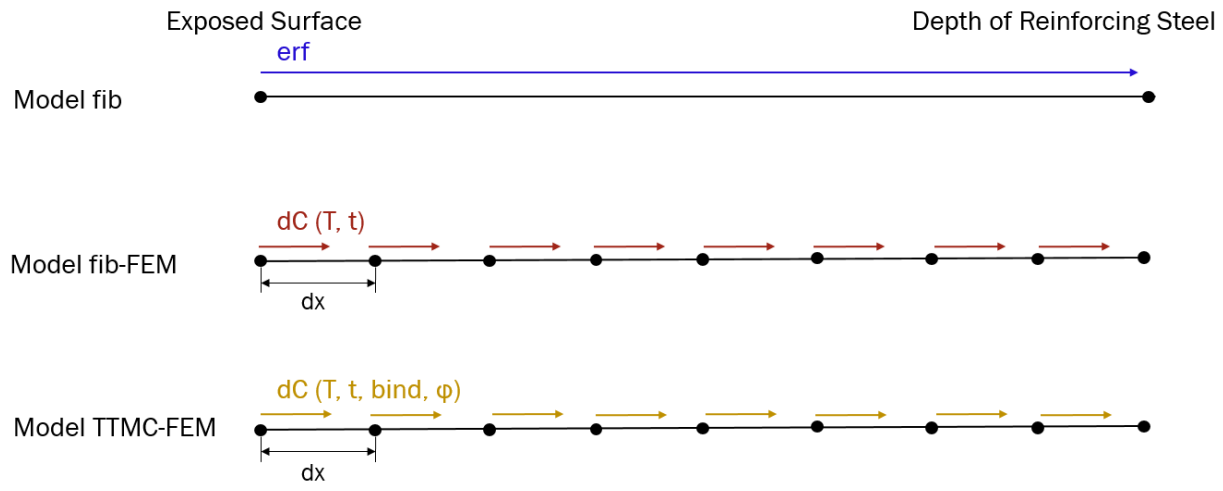

Figure 3: Graphic comparison of three service life models

3.3.4. Mesh Convergence

In Models fib-FEM and TTMC-FEM, the length of the x-mesh influences the chloride concentration at the depth of the rebar due to the finite element solution. If the x-mesh ends at the depth of the rebar, the chlorides 'build-up' artificially at that depth, while in reality, they would continue penetrating past the rebar depth deeper into the concrete. To study the influence of the x-mesh, a mesh convergence study was done on the length of the x-mesh. Models fib-FEM and TTMC-FEM were run with the x-mesh at lengths varying from 10 mm beyond the depth of the reinforcing steel to three times the depth of the reinforcing steel. For reference, the mean of the cover depth of the reinforcing steel is 50 mm. The probability of corrosion initiation using each x-mesh length was recorded.

3.3.5. Monte Carlo

Monte Carlo convergence studies were completed on all three models for any set of input variables to ensure that the sampling was representative and resulted in a converged probability of failure. For each unique set of input variables, the model was run at a variety of samples. The

model was run at each number of samples five times. The coefficient of variation on the probability of failure was computed by Equation 20, shown below

$$\delta_{p_f} = \sqrt{\frac{1 - p_f}{n p_f}} \qquad \text{Equation 20}$$

where p_f is the average probability of failure for a certain number of samples, n. The probability of failure was considered converged if the coefficient of variation on the average probability of failure for the five runs at a certain number of samples was less than 5%. Because the average probability of failure changed with changing input variables in all three models, so did the number of samples required for convergence.

3.3.6. Model Verification

To verify that the models were working correctly, their results were verified against a chloride profile taken from a 17-year-old bridge in Giles, VA (Williamson 2007). The input parameters for this verification bridge can be seen in

Table 2.

Table 2: Input variables for model verification bridge

Variable		Distribution	Mean	Standard Deviation	Source
a	Cover depth, mm	Lognormal	50	6	--
b_e	Regression variable	Normal	4800	700	(fib 2006)
α	Aging factor	Beta	0.3	0.12	(fib 2006)
D_{RMC0}	Rapid migration coefficient, $\frac{mm^2}{year}$	--	17.49	--	(Williamson 2007)
t_o	Reference time, years	--	17	--	
T	Yearly average temperature, K	Normal	285.17	8.12	--
T_{ref}	Reference temperature, K	--	293	--	(fib 2006)
Ci	Initial chloride concentration, $\% \frac{mass\ Cl}{mass\ concrete}$	--	0.3	--	(Williamson 2007)
Cs	Surface chloride concentration, $\% \frac{mass\ Cl}{mass\ concrete}$	--	5.57	--	(Williamson 2007)
R	Universal gas constant, $\frac{kJ}{Kmol}$	--	8.314E-03	--	(Flint 2014)
φ_c	Moisture correction factor	--	0.75		(Flint 2014)
α_{bind}	Non-physical binding parameter	--	8.0	--	(Deng et al. 2013)
β_{bind}	Non-physical binding parameter	--	0.46	--	(Deng et al. 2013)
φ_{max}	Max relative humidity	--	0.95	--	(Liu and Weyers 1998)
φ_{min}	Min relative humidity	---	0.85	--	(Liu and Weyers 1998)

3.3.7. Model Comparison

To compare the performance of the three service life models, each of the models were evaluated for a case study bridge. The input variables describing the case study bridge can be found Table 3. The distributions used for the random variables were either fit to data from the listed source, or chosen at the instruction of the listed source. The case study bridge is located in Lynchburg, VA. The type of reinforcing steel used was multiphased martensitic formable steel (MMFX) which is a low carbon, chromium steel. For each model, the probability of failure, service life distribution, and distribution of chloride concentration at all depths was recorded.

Table 3: Input variables for case study bridge

Variable		Distribution	Justification for Distribution Type	Mean	Variation	Source of Data
a	Cover depth, mm	Lognormal	As instructed by (fib 2006)	50	0.12	VDOT
b_e	Regression variable	Normal	as instructed by (fib 2006)	4800	0.15	(fib 2006)
α	Aging factor	Beta	as instructed by (fib 2006)	0.6	0.25	(fib 2006)
D_{RMC0}	Rapid migration coefficient, $\frac{mm^2}{year}$	Normal	as instructed by (fib 2006)	466.5	.13	VDOT
t_o	Reference time, years (days)	--		.0767 (28)	--	(fib 2006)
T	Yearly average temperature, K	Normal	as instructed by (fib 2006)	286.66	7.98	NCDC
T_{ref}	Reference temperature, K	--		293	--	(fib 2006)
Ci	Initial chloride concentration, $\% \frac{mass\ Cl}{mass\ binder}$	Lognormal	fit to data from testing completed by VDOT	0.034	0.027	VDOT
Ccrit	Critical chloride concentration, $\% \frac{mass\ Cl}{mass\ binder}$	Lognormal	fit to data from testing completed by (Ji et al. 2005)	1.08	0.41	(Ji et al. 2005)
Cs	Surface chloride concentration, $\% \frac{mass\ Cl}{mass\ concrete}$	--	--	0.25	--	(Williamson 2007)
R	Universal gas constant, $\frac{kJ}{Kmol}$	--	--	8.314E-03	--	(Flint 2014)
φ_c	Moisture correction factor	--	--	0.75		(Flint 2014)
α_{bind}	Non-physical binding parameter	--	--	13.0	--	(Deng et al. 2013)
β_{bind}	Non-physical binding parameter	--	--	1.0	--	(Deng et al. 2013)
φ_{max}	Max relative humidity	--	--	0.95	--	(Liu and Weyers 1998)
φ_{min}	Min relative humidity	---	--	0.85	--	(Liu and Weyers 1998)
R	Universal gas constant, $\frac{kJ}{Kmol}$	--	--	8.314E-03	--	(Flint 2014)

3.3.8. Sensitivity Analysis

To complete the sensitivity analysis, each model was run for different cases, each case changing one input variable at a time. For a 'base case,' all input variables remained at their original distributions. Input variables were then changed, one at a time, to their mean value, the mean value plus one standard deviation, and mean value minus one standard deviation. Using the one-at-a-time analysis assumes that the input variables are independent, or that their coupled effects are not significant. (Saassouh and Lounis 2012) assumed that concrete cover, diffusion coefficient, critical chloride threshold, and surface chloride concentration were independent. The other variables considered in this thesis are temperature, aging coefficient, and regression variable. The temperature is independent of the other parameters. While the aging coefficient and regression variables are related to the diffusion coefficient, it was assumed that their coupled effects were not significant.

The probability of failure associated with each case was recorded. To evaluate the sensitivity of the model to each of the input variable cases, the probability of failure for each case was normalized against the probability of failure for the base case.

3.3.9. Regional Comparison

Model fib was run for the case study bridge as if it were to be built in each region to compare the effect the regional exposure conditions have on service life. The model input variables that change with region are temperature and surface chloride concentration. The regional temperatures and surface chloride concentrations are shown in Table 4.

Table 4: Temperature and surface chloride concentration inputs for regional comparison on case study bridge.

Region	Temperature, K		Surface Chloride Concentration, $\% \frac{mass\ Cl}{mass\ binder}$	
	Mean	Standard Deviation	Mean	Standard Deviation
Tidewater	288.2	7.9	0.35	0.23
Eastern Piedmont	287.3	8.2	0.66	0.16
Western Piedmont	285.8	8.0	1.13	0.46
Northern	285.2	8.4	0.84	0.36
Central Mountain	284.8	8.1	0.96	0.61
Southwestern Mountain	285.6	7.8	1.33	0.62

3.4. Life Cycle Cost

Costs associated with plain reinforcing steel and corrosion resistant reinforcing were compared for the service life predictions from the three models. The service life distribution of the case study bridge was evaluated using Model fib with critical chloride thresholds associated with corrosion resistant and plain reinforcing steel. The model input values for these two critical chloride thresholds can be seen in Table 5. The type of corrosion resistant reinforcing steel considered in this LCC work was MMFX.

Table 5: Critical chloride threshold for plain and corrosion resistant reinforcing steel.

Reinforcing Steel Type	Distribution Type	Critical Chloride Threshold, $\% \frac{mass\ Cl}{mass\ binder}$ Mean	Standard Deviation	Source
Plain reinforcing steel	Beta	0.60	0.15	(fib 2006)
Corrosion resistant reinforcing steel	Lognormal	1.08	0.41	(Ji et al. 2005)

Based on the time to end of service life for each reinforcing steel, the equivalent uniform annual cost (EUAC) distribution was calculated. The probability of the cost of plain reinforcing steel and corrosion resistant reinforcing steel, class I (MMFX) was computed based on VDOT bid data from 2015. EUAC was found using Equation 21.

$$EAUC = \frac{NPV}{1 + \frac{1}{\frac{(1+r)^t}{r}}}$$ Equation 21

NPV is net present value, *r* is the discount rate, and *t* is the time over which the EAUC is being considered. For this analysis, *NPV* was the initial cost of the reinforcing steel. This is the only initial cost, as it was assumed that construction and labor costs associated with each type of reinforcing steel were the same. This LCC analysis was also independent of the type of maintenance strategy chosen, only considering reinforcing steel costs. The distribution of cost for both types of reinforcing steel came from VDOT bid tabulations for the year 2015. The discount rate, *r*, can be determined from the real discount rate relating to the interest rate on a treasury or bond with the same analysis time period (Williamson 2007). This interest rate, 1.5%, was found at (OMB 2015), and interest rates here are updated yearly. The time, *t*, is the time, in years, of service life as predicted from the service life models, Model fib, Model fib-FEM, and Model TTMC-FEM for the respective reinforcing steel type. Because the NPV and *t*, time of service life, are stochastic variables, Monte Carlo simulation was completed to develop a distribution of EAUC for each reinforcing steel.

4. RESULTS

This chapter presents and discusses the results from the exposure characterizations, model comparison, and life cycle cost analysis.

4.1. Characterizations

Based on climatic divisions used by the National Climate Data Center, Virginia was divided into six climate regions. The regions, Tidewater, Northern, Easter Piedmont, Western Piedmont, Central Mountain, and Southwestern Mountain can be seen in Figure 1

4.1.1. Exposure Conditions

Temperature

For Model fib and Model fib-FEM, the temperature was modeled as a yearly average and standard deviation. The average and standard deviation of yearly temperature for the regions of Virginia from 1985-2015 is shown in Table 6.

Table 6: Yearly average temperature results

Region	Yearly average temperature, Kelvin (F)	Standard deviation, Kelvin (F)
Tidewater	288.21 (59.10)	7.92 (17.68)
Eastern Piedmont	287.28 (57.43)	8.17 (29.41)
Western Piedmont	286.66 (56.32)	7.98 (28.72)
Northern	285.82 (54.81)	8.41 (30.33)
Central Mountain	285.17 (53.64)	8.12 (29.23)
Southwestern Mountain	284.85 (53.06)	7.86 (28.30)

The warmest region is the Tidewater region, with an average yearly temperature of 59.1 F. The difference between the warmest and the coolest (Southwestern Mountain) is 6.04 F. The results of the nonlinear regression are shown in Table 7. As Model TTMC-FEM accounts for the

seasonal variation of temperature based on monthly averages, the results of the non-linear regression are shown in Table 7.

Table 7: Temperature regression results by region

Region	Sinusoidal Equation Coefficients $T = \mathrm{a}\sin\left(\frac{2\pi}{12}t + c\right) + d$			Adj. R-square Value
	a	c	d	
Tidewater	10.96	0.9608	288.5	0.9983
Eastern Piedmont	11.30	0.9901	287.6	0.9981
Western Piedmont	11.04	0.9961	287.0	0.9975
Northern	11.63	0.9753	286.1	0.9982
Central Mountain	11.63	0.9753	285.1	0.9982
Southwestern Mountain	10.82	0.9966	285.2	0.9969

The adjusted R-square values are all very close to one, indicating the regressions are a good fit for the data. Figure 4 shows the regression plots for all regions.

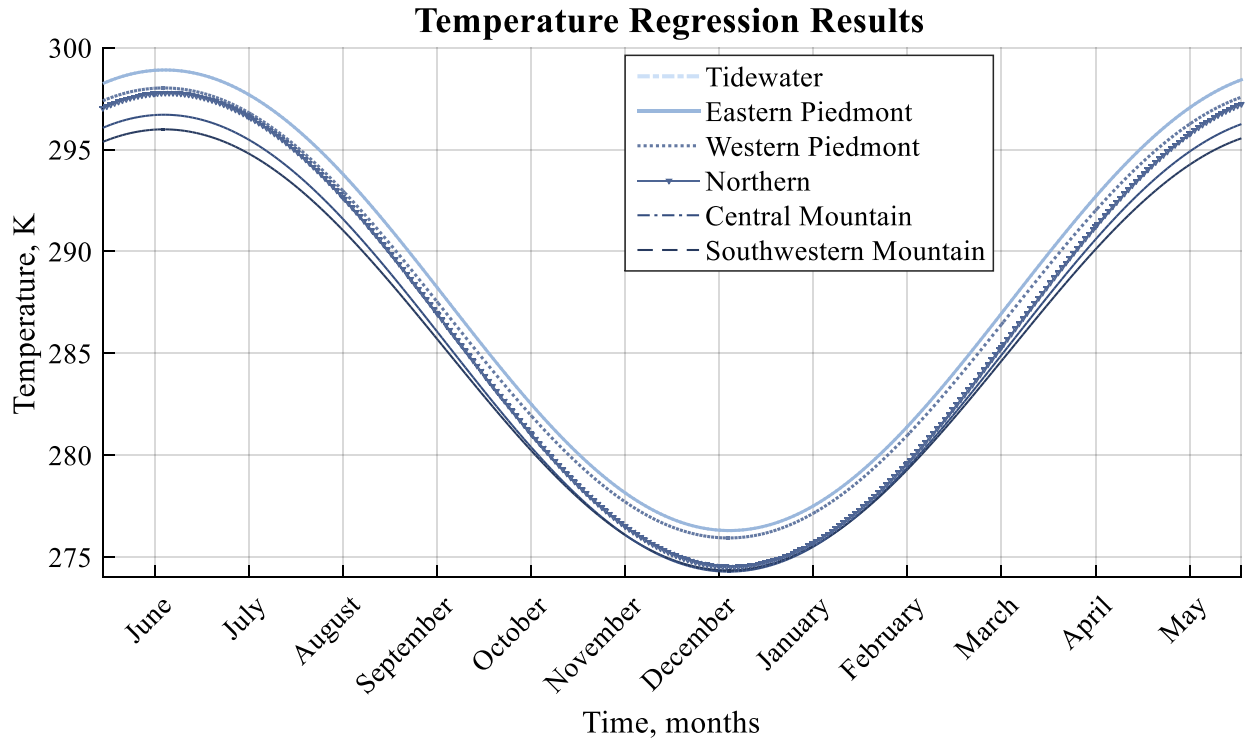

Figure 4: Regional yearly temperature regression results

All six regions have similar yearly temperatures, as shown, but the Tidewater Region has the warmest temperature, on average, year round. The Southwestern Mountain Region has the coolest year round temperature, on average.

The plethora of temperature data available allowed for a very accurate characterization of the yearly temperatures in the regions of Virginia. The accuracy is evident in the adjusted R-square values of the regression equations.

Surface Chloride Concentration

The average and standard deviation of the collected historical surface chloride concentration surveys are shown in Table 8.

Table 8: Compilation of surface chloride concentration results from (Williamson 2007)

Region	Surface Chloride Concentration, $\frac{mass\ Cl}{volume\ concrete}$	
	Mean	Standard Deviation
Tidewater	1.26	0.81
Eastern Piedmont	2.34	0.56
Western Piedmont	4.01	1.63
Northern	2.98	1.30
Central Mountain	3.40	2.16
Southwestern Mountain	4.73	2.19

It is important to note the units of the historical surface chloride concentrations. These measurements were taken on bridges whose cement or binder content was not known, so the mass of chlorides chloride were reported in relation to the volume of concrete. Bridges in the Southwestern Mountain Region had the highest surface chloride concentration while bridges in the Tidewater Region had the lowest.

The results of the fib method for calculating surface chloride concentrations are presented here, and while the results are dissimilar to historical data, they are not unreasonable. The variables necessary for calculating the chloride concentration of the contaminated water due to deicing salts are detailed in Table 9.

Table 9: Results of analysis of meteorological data from winter 2000-2001 including deicing salt application and precipitation results for *fib* method for surface chloride concentration calculation

Region	n, number of salting events per year	$C_{s,i}$, average amount of chloride spread per year, $\frac{g}{m^2}$ (Williamson 2007)	$h_{s,i}$, amount of water from rain and snow during events, mm	C_{oR}, average chloride concentration of contaminated water due to deicing salts, $\frac{g}{l}$
Tidewater	12	38.22	220.99	0.173
Eastern Piedmont	11	90.04	132.74	0.686
Western Piedmont	12	37.37	237.67	0.157
Northern	29	742.22	223.36	3.323
Central Mountain	37	113.99	253.29	0.450
Southwestern Mountain	42	116.88	284.68	0.304

The Northern, Central Mountain, and Southwestern Mountain Regions had the greatest number of salting events and also the greatest amounts of precipitation. The Northern Region had the highest volume of chlorides spread per year because the deicing salt used had a higher concentration of chlorides than the other regions. Because of this high concentration of chlorides, the Northern Region had the highest resulting concentration of the contaminated water. Based on these results, the final surface chloride concentration prediction, $C_{S,\Delta x}$ was calculated for each region, shown in

Table 10.

Table 10: Surface chloride concentration prediction results based on *fib* method

Region	$C_{S,\Delta x}$, $\%\frac{mass\ Cl}{mass\ binder}$
Tidewater	0.25
Eastern Piedmont	0.4
Western Piedmont	0.25
Northern	0.80
Central Mountain	0.35
Southwestern Mountain	0.30

These surface chloride concentrations were reported as the percentage of binder content because the calculation involved is based on the binder content of the concrete. The Western Piedmont conditions resulted in the highest surface chloride concentration and the Eastern Piedmont Region conditions resulted in the lowest.

When comparing the *fib* method surface chloride concentrations to the historical data results, the units must first be made similar. To convert the historical data to % mass binder from % volume concrete, a binder content of 300 $\frac{kg}{m^3}$ was assumed. The results of the converted historic data as compared to the *fib* method surface chloride concentrations are shown in Table 11.

Table 11: Comparison of historical and fib method surface chloride concentrations

Region	Historic, $\%\frac{mass\ Cl}{mass\ binder}$	*fib* Method, $\%\frac{mass\ Cl}{mass\ binder}$	Relative Difference
Tidewater	0.42	0.25	41%
Eastern Piedmont	0.78	0.4	49%
Western Piedmont	1.33	0.25	81%
Northern	0.99	0.80	20%
Central Mountain	0.72	0.35	69%
Southwestern Mountain	1.57	0.30	79%

The range of differences between the two sets of surface chloride concentrations is highly variable, ranging from 22% to 137% different. There are several possible reasons for the high variation. One assumption that effects these results was the assumption of binder content for the

historic bridges. Comparing the *fib* method surface chloride concentrations to historical data for which the binder content is known would be a fairer comparison. The *fib* method for predicting surface chloride concentrations is not easy to follow or detailed in a repeatable manner. In this work, the assumptions made during the calculation of the number of salting events and the amount of water from rain and snow during the events influence the difference in the two surface chloride concentrations. The temperature ranges for which deicing events were defined may not have been VDOT procedure in the past, resulting in differences between the actual amount of days deicing materials were applied and the predicted number of days. The snow-to-liquid ratio used in this work only accounts for air temperature, a more accurate conversion between snow depth and amount of precipitation could be used to account for more than just air temperature. An additional reason for the large differences between the two surface chloride concentration results is the *fib* instructions for converting between the chloride concentration of contaminated solution at the surface to the surface chloride concentration in the concrete are very ambiguous. The interpretation of these instructions could change the results drastically.

Although the *fib* surface chloride concentration predictions differ from historical data, the surface chloride concentrations on bridge decks are highly variable. So, it can be concluded that predicting surface chloride concentrations on bridge decks can be done based on the number of deicing events and precipitation, but more research efforts should be focused on refining the methodology.

4.1.2. Concrete characteristics

Initial Chloride Concentration

The initial chloride concentration titration test results, as completed by the Virginia Department of Transportation (VDOT), are shown in Table 12.

Table 12: VDOT Initial chloride concentration results

Bridge	Initial Chloride Concentration, $\% \frac{mass\ Cl}{mass\ binder}$	Average	Standard Deviation
N&W Railway	0.023 0.036 0.040	0.033	0.009
Wolf Creek	0.026 0.026 0.021	0.024	0.003
Richmond	0.005 0.005 0.004	0.004	0.000
Herring Creek	0.052 0.033 0.054	0.046	0.011
Herring Creek	0.062 0.060 0.062	0.061	0.001

Only the bridges listed provided samples available for initial chloride concentration testing. The concrete from The Richmond bridge had the lowest initial chloride concentration while the Herring Creek bridge had the highest initial chloride concentration.

The average initial chloride concentration was equal to 0.034 % mass binder, with a standard deviation of 0.021 % mass binder. While the standard deviation of initial chloride concentrations between samples from a single bridge were small, the overall standard deviation was large. The variation between initial chloride concentrations for different bridges was variable: the initial chloride concentration of the concrete from Richmond was an order of magnitude smaller than the results from the other bridges. More testing of concrete mixes from different concrete

suppliers used in Virginia and from different regions of the state would provide a useful database for service life modeling.

Chloride Migration Coefficient

The VDOT results for the NT Build 492 tests at 28 days are shown below in Table 13. These results are from the bridge used in the case study model comparison. A total of nine samples underwent NT Build 492 testing.

Table 13: 28-Day VDOT NT Build 492 test results for case study bridge

	Chloride Migration Coefficient, $\frac{mm^2}{year}$
Test Results	473.45
	394.48
	389.00
	515.67
	423.22
	547.92
	527.42
	429.95
	497.71
Average	466.54
Standard Deviation	59.35

The *fib* Bulletin instructs that a standard deviation equal to 20% of the mean is to be used for the standard deviation of the chloride migration coefficient. The standard deviation of the results from the VDOT tests, 59.35 $\frac{mm^2}{year}$, was less than 20% of the mean which would be equal to 93.31 $\frac{mm^2}{year}$. The actual, experimentally-derived, standard deviation was used in the service life models.

Completion of more NT Build 492 tests in Virginia could show that a smaller standard deviation is the norm, not the exception. This should be completed in the future to understand fully the

variation associated with the chloride migration coefficients resulting from the NT Build 492 tests as they are completed in VDOT laboratories.

4.2. Service Life Models

4.2.1. Mesh Convergence

Figure 5 and Figure 6 show the how the probability of corrosion initiation was affected by the x-mesh length. The x-mesh length was varied from the surface to between 150 mm and 50 mm deep. The probability of corrosion initiation for each x-mesh length was normalized against the probability of corrosion initiation, $p_{CI,}$ for an x-mesh length of 150 mm.

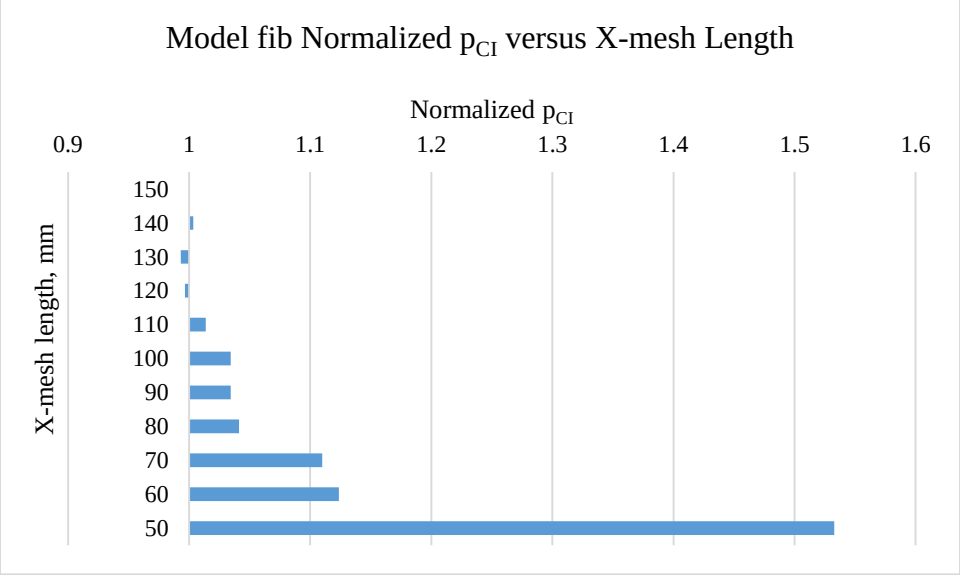

Figure 5: X-mesh influence on p_{CI} Model fib-FEM

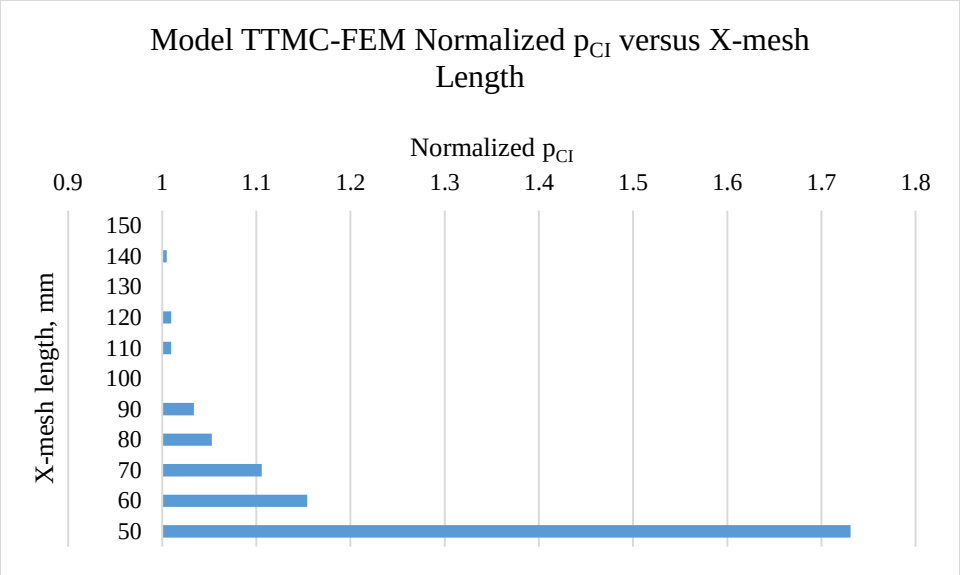

Figure 6: X-mesh influence on p_{CI} Model TTMC-FEM

In Model fib-FEM, the probability of corrosion initiation changes by more than 10% at an x-mesh length of 70 mm. In Model TTMC-FEM, the probability of corrosion initiation changes by more than 10% again at an x-mesh length of 70 mm. For reference, the mean depth of the reinforcing steel was 50 mm. The x-mesh length of 100 mm was used in the service life models, Model fib-FEM and Model TTMC-FEM, to balance computational expense and avoid the effects of the x-mesh length influencing the probability of corrosion initiation.

4.2.2. Monte Carlo Convergence

Table 14 shows the number of Monte Carlo simulations, *n*, completed and the average probability of corrosion initiation, p_{CI}, from the five runs associated with each model. Also shown is the coefficient of variation on the probability of corrosion initiation estimator, $\delta_{p_{CI}}$.

Table 14: Monte Carlo convergence results

Model	n	Average p_{CI}	$\delta_{p_{CI}}$
fib	7000	0.05	5.20%
fib-FEM	2000	0.16	5.12%
TTMC-FEM	2000	0.16	5.12%

Model fib required such a large number of samples because the probability of corrosion initiation was small. The computational time for Model fib at 7000 Monte Carlo simulations was 10000 seconds (167 minutes) on a computer with 12 GB RAM and 2.0 GHz CPUs running Matlab R2015a. The computational time for Model fib-FEM at 2000 Monte Carlo simulations was 6000 seconds (100 minutes), and Model TTMC-FEM at 2000 Monte Carlo simulations took 6000 seconds (100 minutes). If completing these simulations for a number of different sets of input variables, the computation time could become prohibitive.

4.2.3. Model Verification

The chloride profiles of the model validation are shown in Figure 7.

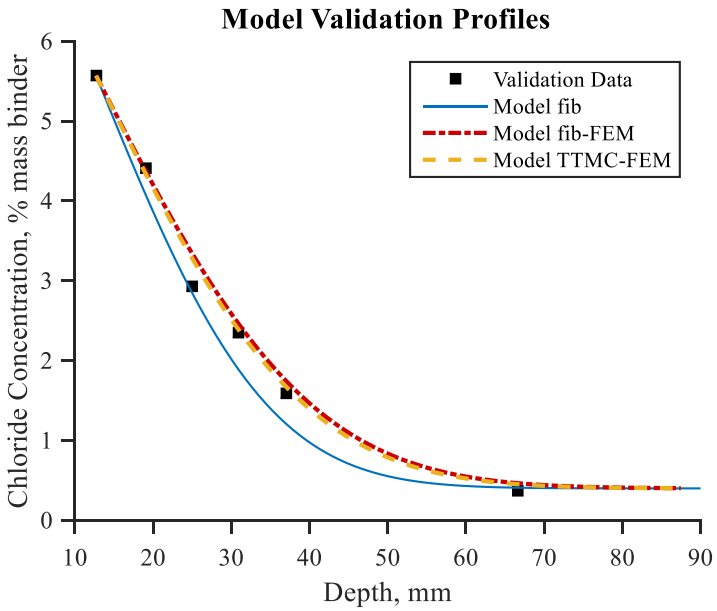

Figure 7: Model validation profiles for 17-year old bridge from (Williamson 2007)

All three models closely match the validation data from the existing structure. However, Model fib-FEM and Model TTMC-FEM seem to match closer than Model fib.

This validation was completed to ensure that the three service life models' results were reasonable when compared to test data from an actual bridge and that the models were working correctly. The apparent diffusion coefficient for the bridge was measured using the chloride profiling method, so this value was used in place of each models' apparent diffusion coefficient calculation.

4.2.4. Model Comparison

For the case study bridge, the estimated probability of corrosion initiation within 100 years and average service life are shown in Table 15 for each model.

Table 15: Estimated probability of corrosion initiation for case study bridge

Model	Estimated Probability of Corrosion Initiation
fib	0.047
fib-FEM	0.162
TTMC-FEM	0.165

Model fib results in the smallest estimated probability of corrosion initiation; it predicts that 95% of the time a bridge deck will reach a service life of 100 years before corrosion initiation. Model fib-FEM and Model TTMC-FEM predict that 84% of the time a bridge deck will reach a service life of 100 years. For the three models, 100 simulations of chloride concentrations versus time are shown below in Figure 8, Figure 9, and Figure 10.

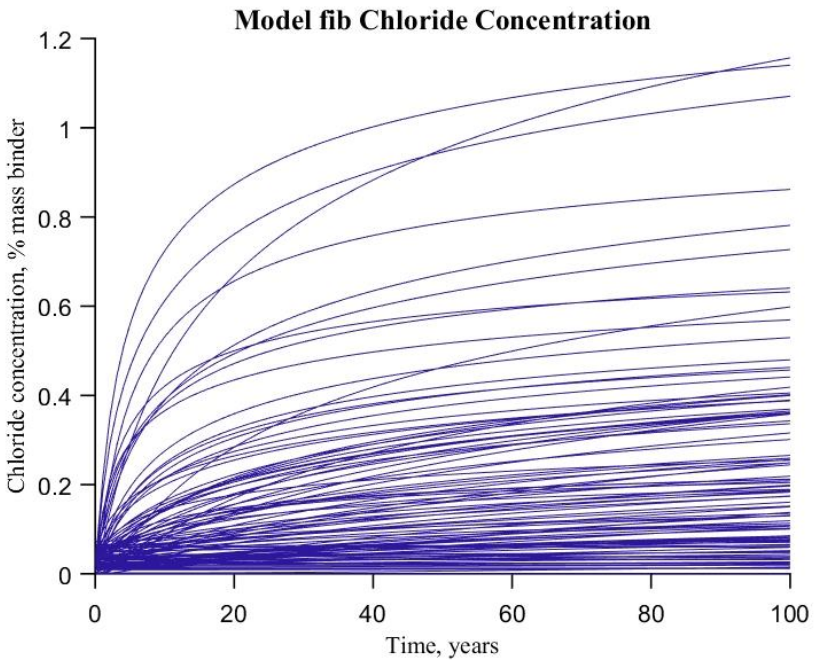

Figure 8: Model fib 100 iterations of chloride concentration at reinforcing steel depth over 100 years for case study bridge

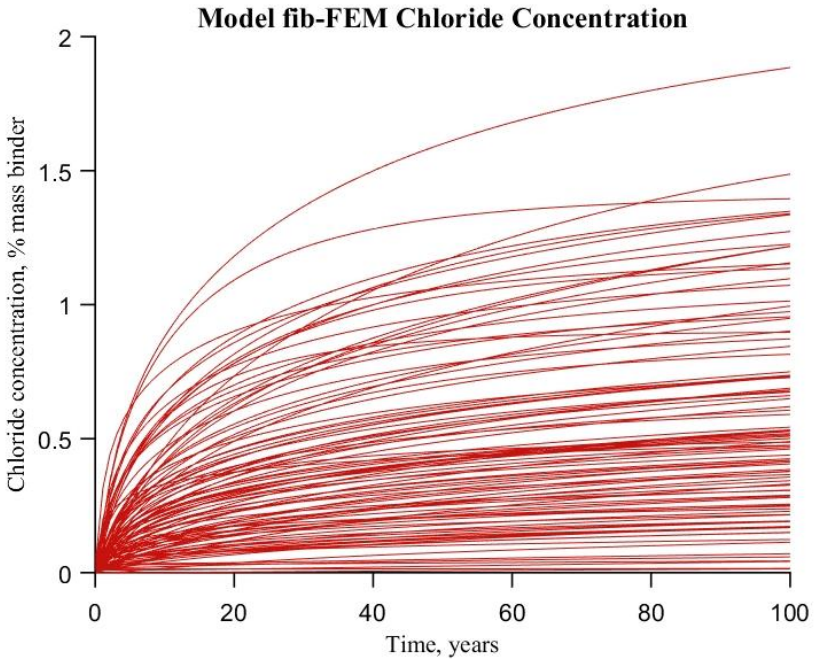

Figure 9: Model fib-FEM 100 iterations of chloride concentration at reinforcing steel depth over 100 years for case study bridge

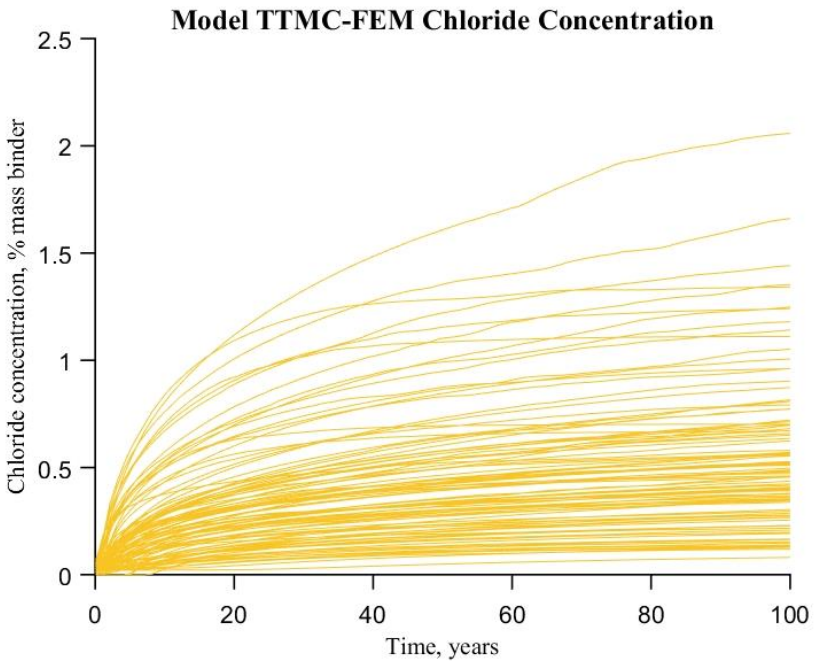

Figure 10: Model TTMC-FEM 100 iterations of chloride concentration at reinforcing steel depth over 100 years for case study bridge

The profiles for Model TTMC-FEM are not as 'smooth' as those from Model fib and Model fib-FEM because of the seasonal variations of temperature and moisture accounted for in Model TTMC-FEM. Profiles obtained from Model fib show more profiles occurring at lower chloride concentrations. The histograms of the chloride concentration at the depth of the reinforcing steel after 100 years are provided in Figure 11.

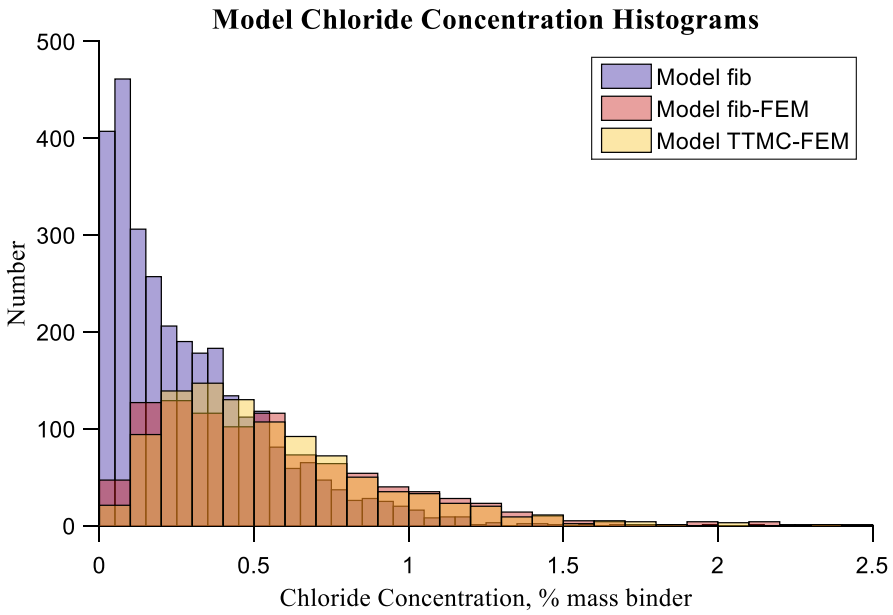

Figure 11: Histograms of chloride concentrations at reinforcing steel depth after 100 years

The estimated probability density functions for the chloride concentration at the depth of the reinforcing steel at 100 years are shown in Figure 12.

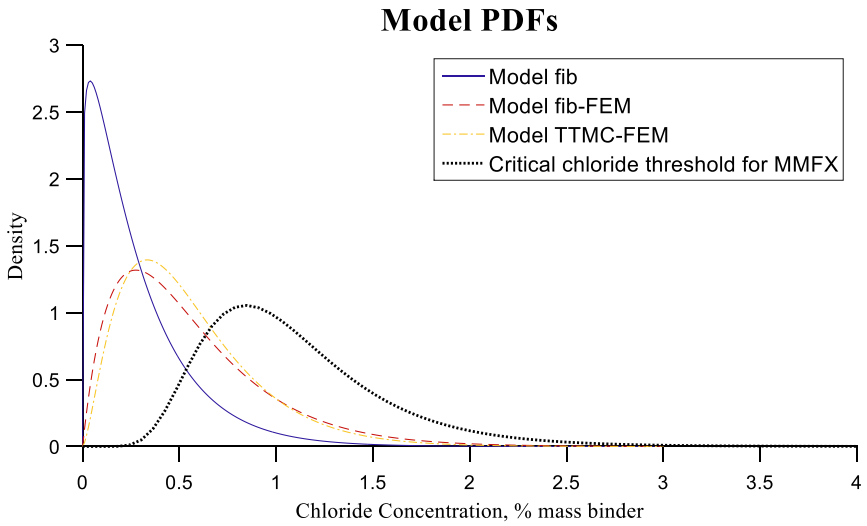

Figure 12: PDFs of service life models compared to critical chloride threshold for MMFX reinforcing

The three model distributions were best represented by two-parameter gamma distributions. The gamma distribution parameters for the models are provided in Table 16. The shape parameters *a* and *b* fully describe the distributions.

Table 16: Model chloride concentration probability density function parameters

Model	Distribution Type	Shape Parameters		Mean, % mass binder		Standard Deviation, % mass binder	
		a	*b*	Sample	Distribution	Sample	Distribution
fib	Gamma	1.1532	0.2532	0.2928	0.2927	0.2675	0.2725
fib-FEM	Gamma	1.9742	0.2822	0.5572	0.5572	0.4010	0.3966
TTMC-FEM	Gamma	2.5140	0.2202	0.5537	0.5537	0.3543	0.3492

The similarities between the sample mean and standard deviation and the distribution mean and standard deviation indicate the gamma functions represent the data well. The PDFs show that, again, Model fib has a higher probability of smaller chloride concentrations, less than 0.5 % mass binder. Model fib-FEM and Model TTMC-FEM are very similar and have greater probabilities associated with higher chloride concentrations.

Compared to Model fib, Models fib-FEM and TTMC-FEM were more conservative in the service life modeling of the case study bridge; they predicted higher chloride concentrations and therefore higher probabilities of corrosion initiation. The difference between the Model fib and Model fib-FEM solutions was significant while the difference between Model fib-FEM and Model TTMC-FEM was much smaller. Model fib estimated a 5% chance of corrosion initiation within 100 years for the service life modeling of the case study bridge. Models fib-FEM and TTMC-FEM predicted the chance of corrosion initiation within 100 years is over three times that of Model fib at 16%. The probabilities of corrosion initiation estimated here apply only to the case study bridge input parameters. In comparing the implementation complexity, Model fib is straightforward, as is Model fib-FEM, although Model fib-FEM is computationally more

complex. Model TTMC-FEM is the most complex to implement and computationally. Since only one case study bridge has been studied, the differences in the models here should not be assumed to apply to a different set of input parameters. If chloride concentration profile data existed for a 100-year exposure period, the models should be validated against that. This validation would allow the quantification of which model most accurately models chloride ingress over 100 years. From the model validation completed in this work, it was inferred that Model fib underestimates service life while Models fib-FEM and TTMC-FEM more correctly estimated service life.

The solutions from Model fib and Model fib-FEM highlight the difference between using the error function solution and the finite element solution. Model fib, the error function solution, underestimated chloride ingress because of the error function solution method's treatment of the apparent diffusion coefficient. The maturation of chloride diffusion is measured theoretically by chloride diffusion tests at different curing ages. In real-world exposure conditions, this maturation occurs while the concrete is exposed to chlorides, and so maturation measured from chloride profiles also includes other effects such as binding. Model fib and Model fib-FEM both attempt to capture more than just aging effects, but the solution methods' treatment of the time-dependent apparent diffusion coefficient differs. The error function solution the solves for the chloride concentration after 100 years as if the apparent diffusion coefficient was always equal to the apparent diffusion coefficient after 100 years. In reality, the diffusion coefficient decreases with age, and Model fib captures this behavior, but the application of the apparent diffusion coefficient when solving for chloride concentration does not match the time-dependent behavior of the apparent diffusion coefficient. The finite element solution does capture the time-dependent behavior in its solution.

The solutions from Model fib-FEM and Model TTMC-FEM highlight the effects of accounting for time-dependent moisture and temperature and binding effects. For the case study bridge, these two models estimated very similar probabilities of corrosion initiation, 16.2% and 16.5%, respectively. Models fib-FEM and TTMC-FEM may not have such similar results for a bridge in a study whose moisture and temperature are less seasonally stable than those observed in Virginia. The time-dependent temperature in Virginia only ranged 12 K from summer to winter months. The moisture content in Virginia bridges is close to 100%, ranging from 85% to 95% (Liu and Weyers 1998), so its effects on chloride diffusion were small.

4.2.5. Sensitivity Analysis

The tornado diagrams below, Figure 13, Figure 14, and Figure 15 show the effect that each stochastic variable had on the probability of corrosion initiation for each model. The tornado diagrams show the normalized probability of corrosion initiation for the mean case, mean plus one standard deviation (high), and mean minus one standard deviation (low).

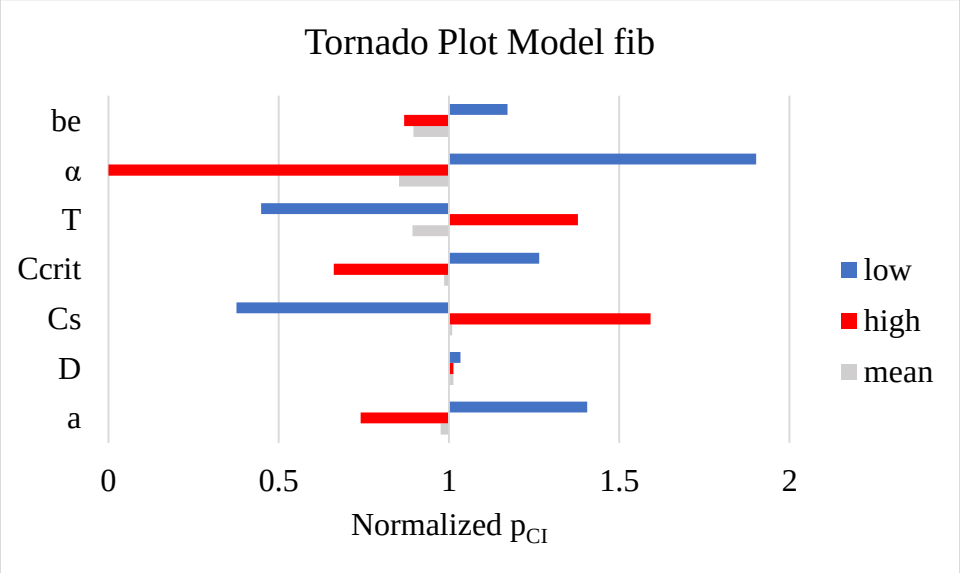

Figure 13: Sensitivity analysis results Model fib

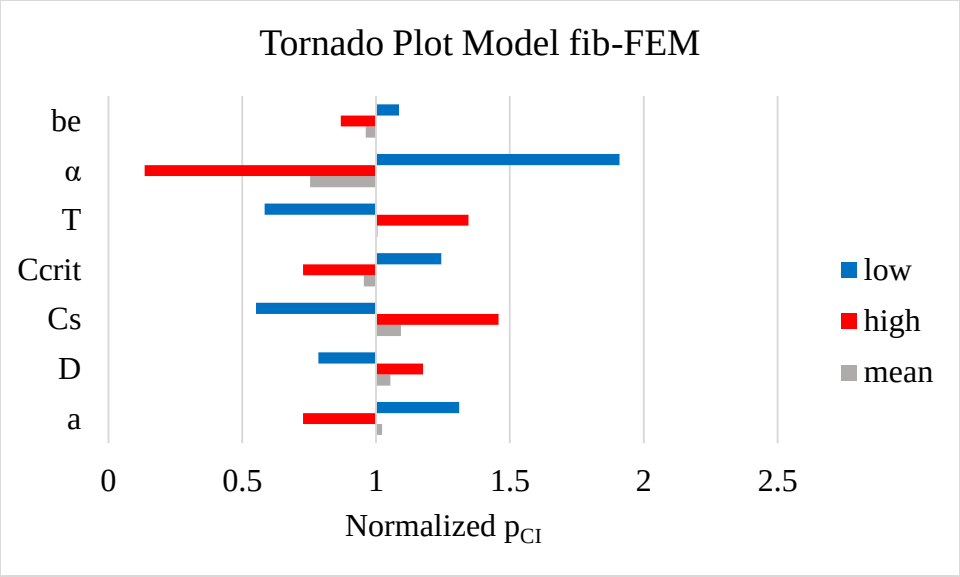

Figure 14: Sensitivity analysis results Model fib-FEM

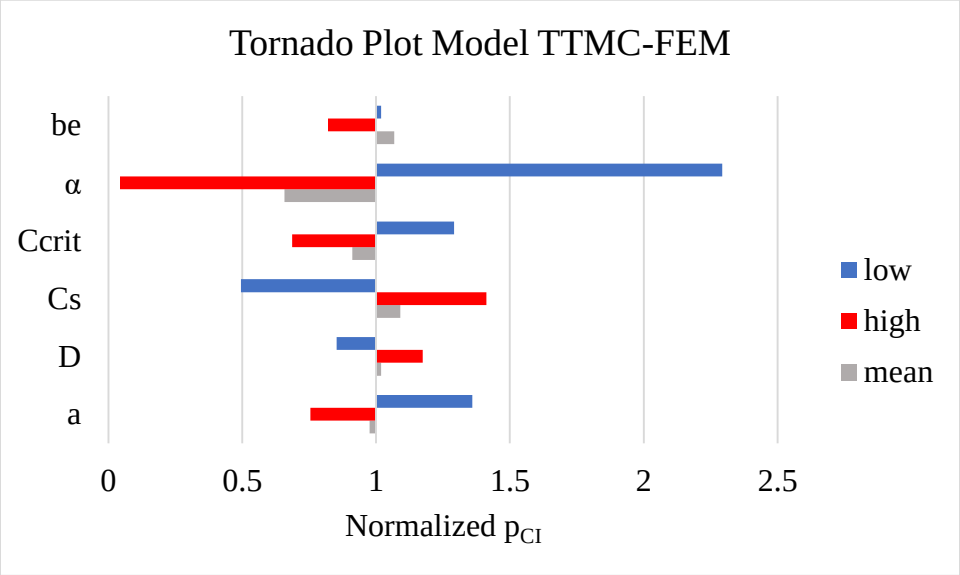

Figure 15: Sensitivity analysis results Model TTMC-FEM

In all three models, the aging coefficient, α, effects the probability of corrosion initiation the most. In Model fib, the surface chloride concentration, Cs, also greatly affects the probability of

corrosion initiation. The temperature, T, also affects the probability of corrosion initiation in Models fib and fib-FEM. The temperature was not included in Model TTMC-FEM's sensitivity analysis as it was not a random variable in that model. In Model TTMC-FEM, the cover depth, a, and the critical chloride threshold, Ccrit, have the same level of influence on the probability of corrosion initiation. In all three models, the non-steady state migration coefficient, D, has the least influence on the probability of corrosion initiation.

Each sensitivity analysis case was influenced by the size of the variables' standard deviation. If a variable has a large standard deviation, it may greatly affect the probability of corrosion initiation, but not necessarily due to model sensitivities to that variable, but due to the size of the standard deviation. Due to this, this sensitivity analysis is most applicable to the model input variables used in this work, as different conditions with different input variables may have different standard deviations, varying the results.

The results of the sensitivity analysis conducted in this thesis were compared to sensitivity analysis results of other service life model research, shown in Table 17.

Table 17: Comparison of sensitivity analysis to other works

Work	Most Important Variable
This Thesis	aging coefficient, α
(Saassouh and Lounis 2012)	surface chloride concentration, Cs
(Boddy et al. 1999)	aging coefficient, m

The results of the sensitivity analysis in this thesis align well with other researchers' results. The two most influential parameters in this work, the aging coefficient and the surface chloride concentration are the most important variables found by other researchers.

4.2.6. Regional Comparison

The resulting estimated probabilities of corrosion initiation from Model fib for the case study bridge modeled as if it were built in each of the regions of Virginia are provided in Table 18.

Table 18: Estimated probability of corrosion initiation for case study bridge if it were built in each region of Virginia

Region	Estimated Probability of Corrosion Initiation
Tidewater	0.0036
Northern	0.0054
Eastern Piedmont	0.0470
Western Piedmont	0.0219
Central Mountain	0.0466
Southwestern Mountain	0.0711

The Southwestern Mountain Region conditions resulted in the largest estimated probability of corrosion initiation of 7.1%. The Tidewater Region conditions resulted in the smallest estimated probability of corrosion initiation of 0.36%, nearly 20 times less than the Southwester Mountain Region.

Figure 16 provides the chloride concentration probability density functions associated with each regional analysis. The parameters of the PDFs and the sample and distribution means and standard deviations are provided in Table 19.

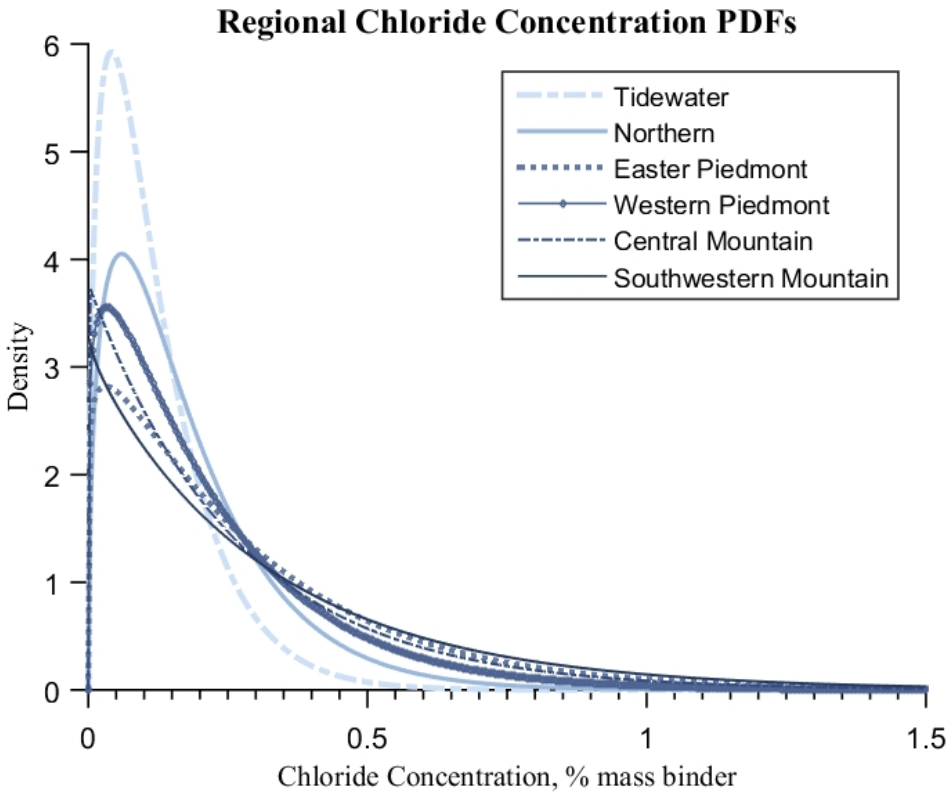

Figure 16: Probability density functions for chloride concentration at the depth of reinforcing steel after 100 years for case study bridge in all Virginia exposure regions

Table 19: Probability density function parameters for regional comparison chloride concentrations at the depth of reinforcing steel after 100 years

Region	Distribution Type	Shape Parameters		Mean, % mass binder		Standard Deviation, % mass binder	
		a	b	Sample	Distribution	Sample	Distribution
Tidewater	gamma	1.5170	0.0807	0.1224	0.1224	0.1105	0.0993
Northern	gamma	1.4996	0.1195	0.1792	0.1792	0.1359	0.1463
Eastern Piedmont	gamma	1.1208	0.2580	0.2892	0.2892	0.2644	0.2731
Western Piedmont	gamma	1.1731	0.1888	0.2214	0.2214	0.2058	0.2044
Central Mountain	gamma	1.0005	0.2641	0.2643	0.2643	0.2989	0.2642
Southwestern Mountain	gamma	0.9788	0.3336	0.3265	0.3265	0.3381	0.3300

All regional chloride concentrations were represented as gamma distributions. The Tidewater Region was predicted to experience the lowest chloride concentration while the Southwester Mountain exposure conditions led to the highest predicted chloride concentrations.

When changing the region, the temperature and surface chloride concentrations were affected. If the surface chloride concentration results from each region were ranked from highest to lowest mean value, the ranking matches the historical surface chloride concentration ranks. This further confirms the results of the sensitivity analysis, as surface chloride concentration affected the estimated probability of corrosion initiation more than the temperature.

If the same bridge deck concrete design were used in different regions of Virginia, the resulting estimated probabilities of corrosion initiation would vary greatly. The case study bridge was planned originally to be constructed in the Eastern Piedmont Region, where Model fib estimated a 4.7% chance of corrosion initiation within 100 years. If constructed in the Tidewater region, Model fib estimated only a 0.36% chance of corrosion initiation. So, because the exposure conditions change with the regions, region-specific designs are necessary to optimize the design.

4.3. Life Cycle Cost

The probability density of the unit cost (per pound) for plain reinforcing and corrosion resistant steel in 2015 is shown in Figure 17.

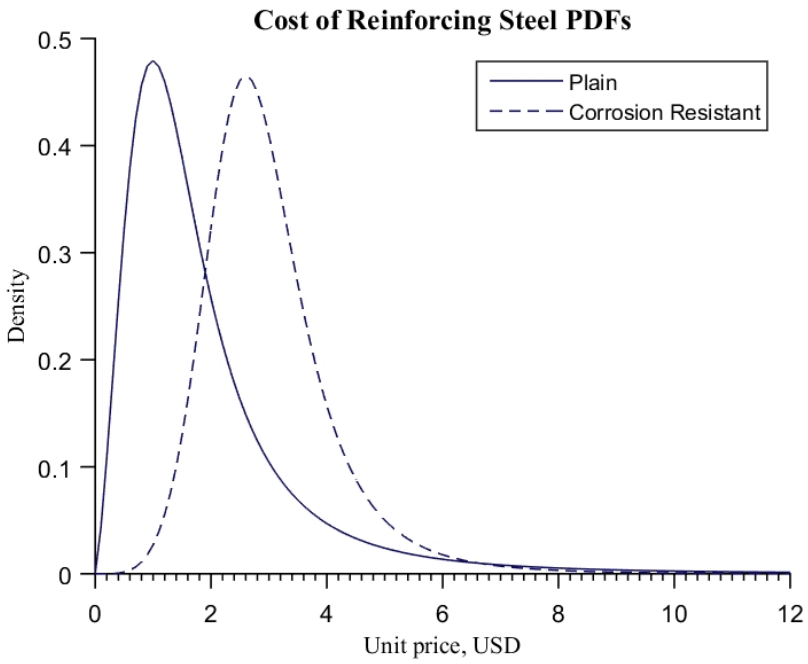

Figure 17: Probability density of reinforcing steel unit cost in 2015

The properties of the probability density function parameters relating to the costs of reinforcing steels are provided in Table 20.

Table 20: Probability density function parameters for reinforcing steel unit costs in 2015

Reinforcing Steel Type	Distribution Type	Mean, USD		Standard Deviation, USD	
		Sample	Distribution	Sample	Distribution
Plain	log-logistic	2.15	2.03	2.23	3.04
Corrosion resistant	log-logistic	3.23	3.01	1.12	1.18

From Figure 13, it is possible to infer that corrosion resistant steel is costlier than plain reinforcing steel. The maximum cost of plain reinforcing steel in 2015 was $9.00 per pound while the maximum cost of corrosion resistant reinforcing steel in 2015 was $12.00 per pound.

The estimated probabilities of corrosion initiation for each type of reinforcing steel is shown in Table 21.

Table 21: Estimated probability of corrosion initiation for each type of reinforcing steel

Model	Corrosion Resistant (MMFX)	Plain
fib	4.7%	14.3%
fib-FEM	16.2%	38.2%
TTMC-FEM	16.5%	38.6%

The probability of corrosion initiation associated with using plain reinforcing steel was higher than with using corrosion resistant.

The probability density of the Equivalent Uniform Annual Cost (EUAC) for both types of reinforcing steel based on the service life predictions of Model fib is shown in Figure 18. The parameters associated with the functions are provided in Table 22.

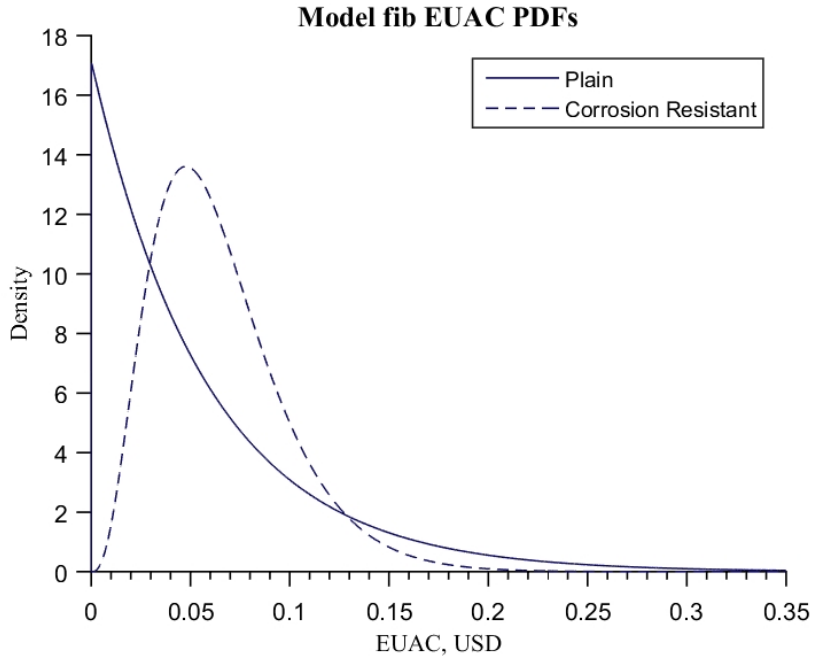

Figure 18: Probability density of EUAC of reinforcing steel based on Model fib

Table 22: Probability density function parameters for reinforcing steel EUAC based on Model fib

Reinforcing Steel Type	Distribution Type	Shape Parameters		Mean, EUAC		Standard Deviation, EUAC	
		a	b	Sample	Distribution	Sample	Distribution
Plain	Gamma	1.0006	0.0582	0.0582	0.0582	0.1876	0.0582
Corrosion Resistant	Gamma	3.8022	0.0170	0.0647	0.0647	0.0965	0.0332

The probability density functions of the Equivalent Uniform Annual Cost (EUAC) for both types of reinforcing steel based on the service life predictions of Model fib-FEM are provided in Figure 19. The parameters associated with the functions are provided in Table 23.

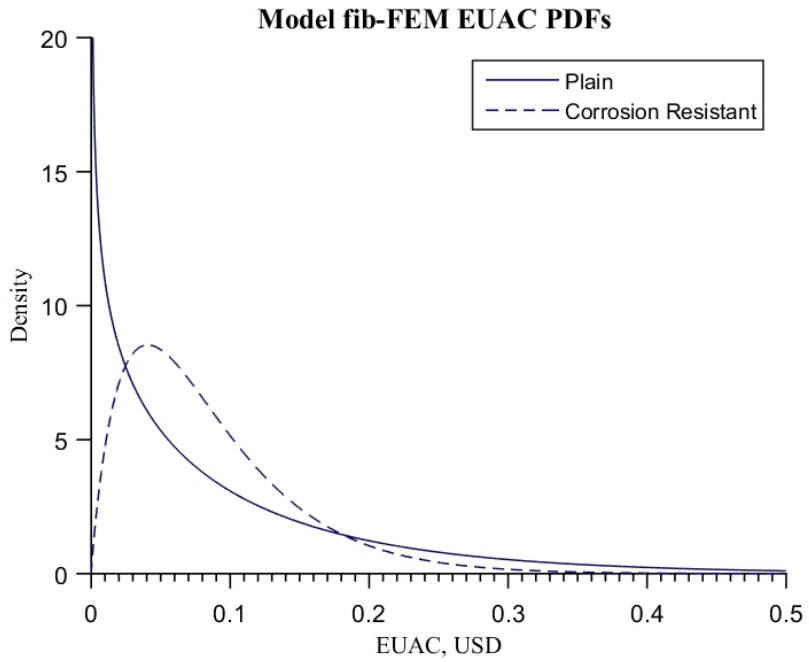

Figure 19: Probability density of EUAC of reinforcing steel based on Model fib-FEM

Table 23: Probability density function parameters for reinforcing steel EUAC based on Model fib-FEM

Reinforcing Steel Type	Distribution Type	Shape Parameters		Mean, EUAC		Standard Deviation, EUAC	
		a	b	Sample	Distribution	Sample	Distribution
Plain	Gamma	0.7410	0.1351	0.1001	0.1000	0.2961	0.1163
Corrosion Resistant	Gamma	1.9054	0.0449	0.0857	0.0857	0.1263	0.0621

The probability density functions of the Equivalent Uniform Annual Cost (EUAC) for both types of reinforcing steel based on the service life predictions of Model TTMC-FEM are provided in Figure 20. The parameters associated with the functions are provided in Table 24.

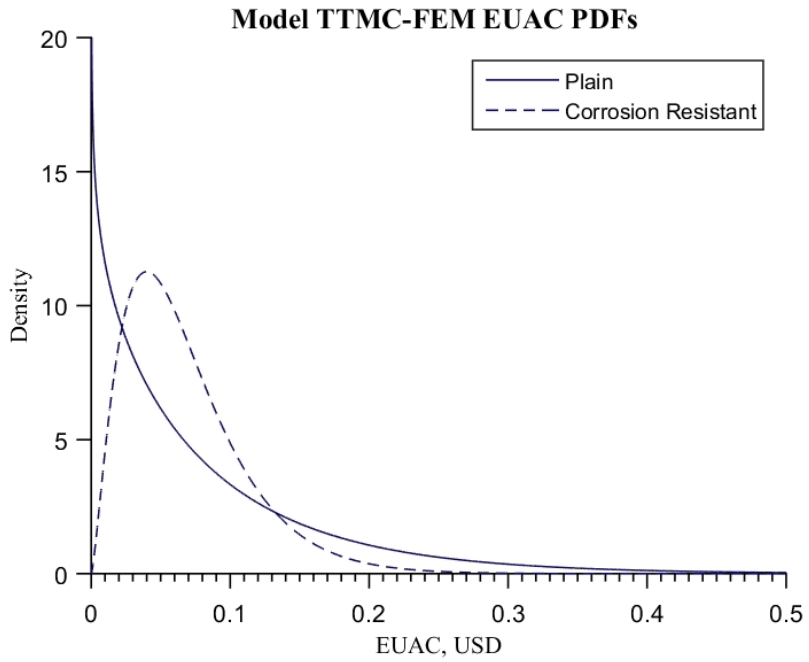

Figure 20: Probability density of EUAC of reinforcing steel based on Model TTMC-FEM

Table 24: Probability density function parameters for reinforcing steel EUAC based on Model TTMC-FEM

Reinforcing Steel Type	Distribution Type	Shape Parameters		Mean, EUAC		Standard Deviation, EUAC	
		a	b	Sample	Distribution	Sample	Distribution
Plain	Gamma	0.8669	0.0955	0.0828	0.0828	0.1757	0.0890
Corrosion Resistant	Gamma	2.4212	0.0280	0.0679	0.0679	0.1155	0.0436

Table 25 provides the probability that the EUAC based on one of the three models for a specific reinforcing steel is less than \$0.05, \$0.10, and \$0.20. For example, P(EUAC) < \$0.05 means the probability that the EUAC is less than \$0.05.

Table 25: Cumulative probabilities associated with EUAC for each reinforcing steel type based on each model

Model	P (EUAC) < \$0.05		P (EUAC) < \$0.10		P (EUAC) < \$0.20	
	Plain	Corrosion Resistant	Plain	Corrosion Resistant	Plain	Corrosion Resistant
fib	57.6%	38.0%	82.0%	86.0%	96.8%	99.8%
fib-FEM	47.0%	33.4%	69.9%	67.7%	95.1%	94.3%
TTMC-FEM	48.1%	40.8%	71.6%	80.3%	92.6%	98.7%

The life cycle cost analysis (LCC) based on the service life predictions from Models fib, fib-FEM, and TTMC-FEM for the two types of reinforcing steel show that underestimating the chloride ingress can underestimate the LCC of the reinforcing steel. The average EUACs of plain and corrosion resistant reinforcing steel based on the estimated service life from Model fib are \$0.058 and \$0.065, respectively. These costs increase by 72% and 32% for plain and corrosion resistant reinforcing steel, respectively, based on Model fib-FEM. The costs increase by 42% and 1% for plain and corrosion resistant reinforcing steel, respectively, based on Model TTMC-FEM. The LCC of the two reinforcing steel types based on Model fib also leads to the conclusion that plain reinforcing steel is more cost effective when only considering initial costs. Models fib-FEM and TTMC-FEM based LCCs show that corrosion resistant reinforcing steel is more likely

to be cost effective, when considering that using plain reinforcing steel results in a much higher probability of corrosion initiation within 100 years. So using a service life model that underestimates chloride ingress, could lead to underestimating LCC.

5. CONCLUSIONS

This chapter summarizes the contributions of this work and highlights the conclusions derived from the studies completed. Also included are areas of future work.

5.1. Characterization

The first major contribution of this work was to characterize the exposure conditions for the regions of Virginia and the concrete mix designs used by the Virginia Department of Transportation (VDOT). The six different exposure regions of Virginia experience a range of temperatures, surface chloride concentrations, precipitation, and deicing conditions as detailed below. The concrete mix design characteristics are discussed below.

5.1.1. Exposure Conditions

Temperature

The exposure regions of Virginia were characterized by temperature based on 30 years of temperature records from the National Climate Data Center. A large amount of historical temperature data allowed for the development of an accurate regression model of the yearly temperature in all regions of Virginia. This model could be used in future service life model predictions. This temperature characterization did not include a warming function that would be associated with climate change; the effects of this could be studied in future characterizations.

Surface chloride concentrations

Although a large amount of historical surface chloride concentration data exists for Virginia bridge decks, this data is often not ideal for use in service life prediction models. The historical surface chloride concentrations came from bridges whose concrete mix designs are unknown.

This makes translating the historical surface chloride concentration into a format for use in service life design models difficult because assumptions must be made about the concrete composition. These assumptions contribute additional uncertainty to an already probabilistic process. Historic surface chloride concentrations were compiled by region and used in the service life models in this work.

The *fib* Bulletin 34 Model Code for Service Life Design method for predicting surface chloride concentrations was completed for the Virginia regions. The *fib* method is not well specified, leading to results that could change drastically based on different assumptions. This method requires knowledge of deicing salt application procedures, precipitation and snow weather records and a conversion factor of snow to liquid ratio. These values are difficult to quantify with confidence for a variety of reasons.

For a better understanding of the number of deicing events, more years should be considered in the future (as only one year was considered here). Analyzing more weather data may reduce variance and provide a more representative value. The snow-to-liquid ratio used in this thesis relied only on temperature; a more detailed future analysis may consider other factors such as altitude and geographic region.

The final step in the *fib* method is to translate the chloride contaminated liquid on the surface of the concrete (from the deicing events and precipitation) to a surface chloride concentration within the surface of the concrete. The *fib* instructions for this step are not complete, and as such, the conversion between the contaminated liquid and the surface chloride concentration was completed using the *fib* example conditions. In the future, ponding tests replicating the conditions a bridge deck would experience from deicing salt applications and precipitation could

be conducted in order to develop a relationship between the chloride contaminated water *on* the concrete with the surface chloride concentration resulting *in* the concrete.

The *fib*-derived surface chloride predictions were not unreasonable when compared to the historical surface chloride concentrations, possibly as a result of the assumption made to complete the method. To mitigate the influence of these assumptions, if historical surface chloride concentrations are available, they are potentially better used as the model's inputs.

5.1.2. Concrete characteristics

Initial Chloride Concentration

Several bridge concrete samples underwent initial chloride concentrations testing at the Virginia Department of Transportation (VDOT). These tests provided an average value of initial chloride concentrations for bridge deck concrete in all of Virginia. The initial chloride concentrations from different concrete mix suppliers were variable. The variability of the initial chloride concentrations should be further quantified for regional concrete suppliers and incorporated in future service life modeling. A better understanding of the variability leads to a more accurate service life model.

Chloride Migration Coefficient

NT Build 492 tests were completed on 28-day concrete samples from one bridge in Virginia. These tests provided the average and standard deviation values of the chloride migration coefficient used in the service life models. Future testing plans should include tests on concrete samples from bridge deck concretes from all regions in Virginia to quantify regional differences and further explore the uncertainty of results from the NT Build 492 tests.

For the bridge deck concrete data used in this work, the standard deviation recorded was less than that suggested by the *fib* service life model. A high standard deviation results in more variability and uncertainty in the service life prediction. In this work, the uncertainty associated with the chloride migration coefficient, and in turn the probability of corrosion initiation, can be decreased by quantifying the standard deviation of test results instead of using the *fib* suggested standard deviation.

5.2. Service Life Model Comparison

The second major contribution of this work was to compare service life predictions from three service life models for a case study bridge in Virginia. Based on the exposure and design characteristics of the case study bridge, the estimated probabilities of corrosion initiation after 100 years of exposure from Model fib, Model fib-FEM, and Model TTMC-FEM were 4.7%, 16.2% and 16.5%, respectively.

While Model fib is straightforward and computationally simple to implement, it underestimates chloride ingress. Model fib-FEM is straightforward, but computationally more complex to implement. Model TTMC-FEM is the most complex and difficult to implement.

For the case study bridge, Models fib-FEM and TTMC-FEM estimated the probability of corrosion initiation after 100 years of exposure was three times greater than estimated by Model fib. Further model validation of surveys over longer time periods could reveal which model most accurately estimates chloride ingress.

The differences in results between Model fib and Model fib-FEM highlight the discrepancies between the error function solution and the finite element solution; the error function solution underestimates chloride ingress. While Model fib accounts for the maturation of the apparent

diffusion coefficient over time, the error function solution uses only one value. The error function solution for chloride concentration after 100 years of exposure solves for chloride concentration as if the apparent diffusion coefficient had been the same over those 100 years. The Model fib-FEM solution uses an apparent diffusion coefficient 'aged' to 100 years and accounts for the time-dependency of the apparent diffusion throughout the solution. Model fib under predicts chloride ingress, possibly leading to a false sense of security in service life modeling and design.

The inclusion of time-dependent temperature and moisture content, as in Model TTMC-FEM, did not greatly affect the probability of corrosion initiation for the case study bridge. This result was attributed to the relatively constant temperature and high humidity in the exposure region of the case study bridge. The yearly temperature in the Eastern Piedmont Region of Virginia is relatively stable, only varying 12 K. The relative humidity in concrete pores in Virginia is high (between 95% and 85%), so the effects of moisture content are not high. In conditions experiencing a much more variable yearly temperature and lower relative humidity, the differences between Model fib-FEM and Model TTMC-FEM would be increased.

Based on the studies completed in this work, it is concluded that Model fib under predicts chloride ingress, overestimating the estimated service life. Model fib-FEM balances solution accuracy and complexity best between the three service life models compared in this work.

5.2.1. Sensitivity Analysis

A sensitivity analysis was completed on each of the service life models to evaluate which input parameter most significantly affects the probability of corrosion initiation. The aging coefficient affected the probability of corrosion initiation most in all three models. The second most

influential variable in the models was surface chloride concentration. The least influential variable was the chloride migration coefficient. This is counter-intuitive, but the influence of the maturation of the migration coefficient is more influential, especially given the low standard of deviation of the chloride migration coefficient observed in the testing. The results of this thesis' sensitivity analysis align with previous service life model sensitivity study results.

Surface chloride concentration and the maturation, or aging, coefficient are the most influential model parameters, and as such, great care should be taken to describe these random variables fully. Future research in this field should delve into better understanding these variables because reducing their variability will most greatly reduce the variability of the probability of corrosion initiation.

5.2.2. Regional Comparison

When ranking the probabilities of corrosion initiation estimated by Model fib for the case study bridge as if it were built in each of Virginia's six regions, the rankings were the same as the rankings of historical surface chloride concentration by region. That is, the regions with the highest surface chloride concentrations also had the highest probability of corrosion initiation. This further validates the results of the sensitivity analysis in that surface chloride concentration is more influential than temperature. In the region the case study bridge is to be constructed (Eastern Piedmont), the probability of corrosion initiation is 20 times higher than the Tidewater Region. So, the regional exposures in Virginia are varied enough to encourage region-specific designs.

5.3. Life Cycle Cost

The final contribution of this work was a life cycle cost analysis. The estimated uniform annual cost (EUAC) for plain and corrosion resistant reinforcing steel over the estimated service life of the case study bridge by the three models were compared. Based on the service life estimated by Model fib, plain reinforcing steel was more cost effective than corrosion resistant reinforcing steel. However, the EUAC associated with plain reinforcing steel based on the service life estimated by Model fib-FEM was 72% higher than Model fib. Based on the service life predicted by Model fib-FEM and TTMC, corrosion resistant reinforcing steel is more cost effective than plain reinforcing steel.

So, underestimating chloride ingress and service life can lead to underestimating the life cycle costs of reinforcing steel (by as much as 72% for the case study bridge). The overestimated service life can also lead to choosing plain reinforcing steel because it seems like the cost effective option. However, corrosion resistant reinforcing steel was more cost effective based on the more accurate service life predictions from Model fib-FEM and Model TTMC-FEM.

5.4. Overall Contributions and Findings

The overall contributions of this thesis are

- characterization of Virginia temperatures;
- comparison of historical surface chloride concentrations to *fib* method for predicting surface chloride concentration;
- characterization of concrete mix design properties relating to the case study bridge used in this thesis;
- comparison of three service life models, Model fib, Model fib-FEM, and Model TTMC-FEM for a case study bridge;

- sensitivity analysis of three service life models; and
- life cycle cost analysis for corrosion resistant reinforcing steel and plain reinforcing steel based on service life predictions.

The significances of these findings are

- the temperature in Virginia has been characterized and made ready for use in further service life designs;
- the differences between historical and *fib* predicted surface chloride concentrations are not extreme, but the *fib* method is ill-constrained;
- initial chlorides in Virginia were highly variable between concrete suppliers, so this variable should be quantified from applicable suppliers for service life designs;
- chloride migration coefficient testing resulted in a standard deviation less than *fib* suggested value, so testing could be completed for lessening uncertainty in the service life model to predict more accurately service life;
- Model fib underestimates chloride ingress, providing a false sense of security for service life designs;
- Models' fib-FEM and TTMC-FEM results are similar in regions where the yearly temperature is not highly variable between seasons and where the relative humidity in the concrete is high;
- the most important variables to quantify in service life models are the surface chloride concentrations and the aging coefficient for the apparent diffusion coefficient,
- service life design should be completed for region-specific exposure conditions to avoid over or under-designing; and

- the underestimation of chloride ingress from Model fib leads to underestimation of life cycle costs of reinforcing steel, by up to 72% for the case study bridge.

In summary, this thesis showed: the importance of characterizing region-specific exposure conditions, that the error function solution underestimates chloride ingress – overestimating service life, and that the overestimation of service life can greatly underestimate life cycle costs. This thesis has shown it is imperative to model correctly the service life of bridge decks to reap the benefits of the service life design.

6. REFERENCES

Andrade, C., Castellote, M., and d'Andrea, R. (2011). "Measurement of ageing effect on chloride diffusion coefficients in cementitious matrices." *Journal of Nuclear Materials*, 412(1), 209-216.

Bagheri, A. R., and Zanganeh, H. (2012). "Comparison of rapid tests for evaluation of chloride resistance of concretes with supplementary cementitious materials." *Journal of Materials in Civil Engineering*, 24(9), 1175-1182.

Bamforth, P. (1999). "The derivation of input data for modelling chloride ingress from eight-year UK coastal exposure trials." *Magazine of Concrete Research*, 51(2), 87-96.

Bastidas-Arteaga, E., Chateauneuf, A., Sánchez-Silva, M., Bressolette, P., and Schoefs, F. (2011). "A comprehensive probabilistic model of chloride ingress in unsaturated concrete." *Engineering Structures*, 33(3), 720-730.

Baxter, M. A., Graves, C. E., and Moore, J. T. (2005). "A climatology of snow-to-liquid ratio for the contiguous United States." *Weather and Forecasting*, 20(5), 729-744.

Bažant, Z., and Najjar, L. (1971). "Drying of concrete as a nonlinear diffusion problem." *Cement and Concrete Research*, 1(5), 461-473.

Boddy, A., Bentz, E., Thomas, M., and Hooton, R. (1999). "An overview and sensitivity study of a multimechanistic chloride transport model." *Cement and concrete research*, 29(6), 827-837.

Cady, P. D., and Weyers, R. E. (1983). "Chloride penetration and the deterioration of concrete bridge decks." *Cement, concrete and aggregates*, 5(2), 81-87.

Deng, D., Shi, C., and De Schutter, G. (2013). "Chloride binding isotherm from migration and diffusion tests." *Journal of Wuhan University of Technology-Mater. Sci. Ed.*, 28(3), 548-556.

fib (2006). "Model code for service life design." *Bulletin 34*.

Flint, M. M. (2014). "A Modular Framework for Performance-based Durability Engineering." Stanford University.

FWHA (2015). "Improving Transportation Investment Decisions Through Life-Cycle Cost Analysis." <https://www.fhwa.dot.gov/infrastructure/asstmgmt/lccafact.cfm>.

Hurley, M., and Scully, J. (2006). "Threshold chloride concentrations of selected corrosion-resistant rebar materials compared to carbon steel." *Corrosion*, 62(10), 892-904.

Ji, J., Darwin, D., Browning, J. P., and Dakota, S. (2005). *Corrosion resistance of duplex stainless steels and MMFX microcomposite steel for reinforced concrete bridge decks*, University of Kansas Center for Research, Incorporated.

Kirkpatrick, T. J. (2001). "Impact of specification changes on chloride induced corrosion service life of virginia bridge decks." Virginia Polytechnic Institute and State University.

Koch, G. H., Brongers, M. P., Thompson, N. G., Virmani, Y. P., and Payer, J. H. (2002). "Corrosion Cost and Preventive Strategies in the United States." FHWA.

Kyle, J., and Wesley, D. (1997). "New conversion table for snowfall to estimated meltwater: Is it appropriate in the High Plains." *Central Region ARP*, 18-04.

Liu, T., and Weyers, R. (1998). "Modeling the dynamic corrosion process in chloride contaminated concrete structures." *Cement and Concrete Research*, 28(3), 365-379.

Luping, T., and Gulikers, J. (2007). "On the mathematics of time-dependent apparent chloride diffusion coefficient in concrete." *Cement and Concrete Research*, 37(4), 589-595.

Mangat, P. S., and Molloy, B. T. (1994). "Prediction of long term chloride concentration in concrete." *Materials and Structures*, 27(6), 338-346.
Martın-Pérez, B., Pantazopoulou, S., and Thomas, M. (2001). "Numerical solution of mass transport equations in concrete structures." *Computers & Structures*, 79(13), 1251-1264.
Martın-Pérez, B., Zibara, H., Hooton, R., and Thomas, M. (2000). "A study of the effect of chloride binding on service life predictions." *Cement and Concrete Research*, 30(8), 1215-1223.
NOAA "U.S. Climate Divisions." <http://www.ncdc.noaa.gov/monitoring-references/maps/us-climate-divisions.php>.
Nokken, M., Boddy, A., Hooton, R. D., and Thomas, M. D. A. (2006). "Time dependent diffusion in concrete—three laboratory studies." *Cement and Concrete Research*, 36(1), 200-207.
NordTest (1999). "492." *Chloride migration coefficient from non-steady-state migration experiments, NT Build 492*.
OMB (2015). "Discount Rates for Cost-Effectiveness, Lease Purchase, and Related Analyses."https://www.whitehouse.gov/omb/circulars_a094/a94_appx-c.
Poulsen, E., and Mejlbro, L. (2010). *Diffusion of chloride in concrete: theory and application*, CRC Press.
Saassouh, B., and Lounis, Z. (2012). "Probabilistic modeling of chloride-induced corrosion in concrete structures using first-and second-order reliability methods." *Cement and Concrete Composites*, 34(9), 1082-1093.
Saetta, A. V., Scotta, R. V., and Vitaliani, R. V. (1993). "Analysis of chloride diffusion into partially saturated concrete." *ACI Materials Journal*, 90(5).
Stanish, K., Hooton, R. D., and Thomas, M. (2001). "Testing the chloride penetration resistance of concrete: a literature review." *2001*.
Stewart, M. G. (2001). "Reliability-based assessment of ageing bridges using risk ranking and life cycle cost decision analyses." *Reliability Engineering & System Safety*, 74(3), 263-273.
Tang, L. (1996). "Chloride Penetration into the Concrete Exposed Under Different Conditions." *7th International Conference on the Durability of Building Materials and Components*Stockholm.
VDOT (2015). "State of the Structures and Bridges Report." S. a. B. Division, ed.
Williamson, G., Weyers, R. E., Brown, M. C., and Sprinkel, M. M. (2007). "Bridge Service Life Prediction and Cost." Virginia Department of Transportation, Virginia Transportation Research Council, 77.
Williamson, G. S. (2007). "Service Life Modeling of Virginia Bridge Decks."

APPENDIX A

Table 26: Virginia weather stations used for temperature characterization

Region Number	NCDC Station Name
1	CORBIN VA US
1	DISPUTANTA VA US
1	SANDSTON VA US
1	OCEANA NAS VA US
1	SUFFOLK LAKE KILBY VA US
1	FENTRESS NAVAL AUXILIARY FIELD VA US
1	EASTVILLE VA US
1	WAKEFIELD MUNICIPAL AIRPORT VA US
1	WILLIAMSBURG 2 N VA US
1	GREAT DISMAL NWR VIRGINIA VA US
1	NORFOLK INTERNATIONAL AIRPORT VA US
1	NORFOLK SOUTH VA US
1	JAMES RIVER VIRGINIA VA US
1	SOMERSET VA US
1	MANASSAS VA US
1	PETERSBURG VA US
1	NORFOLK NAS VA US
1	HOPEWELL VA US
1	NEWPORT NEWS INTERNATIONAL AIRPORT VA US
1	WALLOPS ISLAND WALLOPS FLIGHT FACILITY VA US
1	WAKEFIELD 1 NW VA US
1	STONY CREEK 2 N VA US
1	PAINTER 2 W VA US
1	EMPORIA 1 WNW VA US
1	HOLLAND 1 E VA US
2	AMELIA 4 SW VA US
2	FREDERICKSBURG SEWAGE VA US
2	JOHN H KERR DAM VA US
2	ASHLAND HANOVER CO MUNICIPAL AIRPORT VA US
2	ASHLAND VA US
2	WEST POINT 2 NW VA US
2	LOUISA VA US
2	CLARKSVILLE VA US
2	FARMVILLE 2 N VA US
2	CROZIER VA US
2	BREMO BLUFF VA US

2	CAMP PICKETT VA US
3	FREE UNION VA US
3	PHILPOTT DAM 2 VA US
3	SOUTH BOSTON VA US
3	MEADOWS OF DAN 5 SW VA US
3	TYE RIVER 1 SE VA US
3	STUART VA US
3	MONTEBELLO FISH HATCHERY VA US
3	CHARLOTTESVILLE 2 SSE VA US
3	CHARLOTTESVILLE 2 W VA US
3	ROCKY MOUNT VA US
3	BROOKNEAL VA US
3	DANVILLE REGIONAL AIRPORT VA US
3	MONTICELLO VA US
3	MARTINSVILLE FLT PLANT VA US
3	CHARLOTTE COURT HOUSE VA US
3	LYNCHBURG REGIONAL AIRPORT VA US
3	CHARLOTTESVILLE ALBEMARLE AIRPORT VA US
3	CHATHAM VA US
3	APPOMATTOX VA US
4	BOSTON 4 SE VA US
4	VIENNA VA US
4	PIEDMONT RESEARCH STATION VA US
4	QUANTICO MCAS VA US
4	MOUNT WEATHER VA US
4	WOODSTOCK 2 NE VA US
4	RICHMOND INTERNATIONAL AIRPORT VA US
4	SPERRYVILLE VA US
4	LINCOLN VA US
4	WASHINGTON DC DULLES INTERNATIONAL AIRPORT VA US
4	MADISON VA US
4	CAPE CHARLES 5 ENE VA US
4	EDINBURG VA US
4	WARRENTON 3 SE VA US
4	WINCHESTER 7 SE VA US
4	WINCHESTER VA US
4	FRONT ROYAL VA US
4	LURAY 5 E VA US
4	STERLING RCS VA US
4	FORT VALLEY VIRGINIA VA US
5	LIME KILN VIRGINIA VA US
5	MUSTOE 1 SW VA US
5	MILLGAP 2 NNW VA US

5	STAUNTON WATER TREATMENT PLANT VA US
5	HOT SPRINGS VA US
5	GATHRIGHT DAM VA US
5	ROANOKE REGIONAL AIRPORT VA US
5	LEXINGTON VA US
5	DALE ENTERPRISE VA US
5	COVINGTON FILTER PLANT VA US
5	WAYNESBORO WATER TREATMENT VA US
5	CRAIG VALLEY VIRGINIA VA US
5	ROANOKE 8 N VA US
6	NORTH FORK LAKE VA US
6	CLINTWOOD 1 W VA US
6	BIG STONE GAP VA US
6	PULASKI VA US
6	LEBANON VA US
6	JOHN FLANNAGAN LAKE VA US
6	WYTHEVILLE VA US
6	SALTVILLE 1 N VA US
6	GALAX RADIO WBRF VA US
6	GALAX WATER PLANT VA US
6	COPPER HILL VA US
6	ABINGDON 3 S VA US
6	NORA 4 SSE VA US
6	RADFROD 3 N VA US
6	GRUNDY VA US
6	WISE VIRGINIA VA US
6	RICHLANDS VA US
6	STAFFORDSVILLE 3 ENE VA US
6	BLACKSBURG NATIONAL WEATHER SERVICE OFFICE VA US
6	CHRISTIANSBURG VA US
6	WISE 3 E VA US
6	BURKES GARDEN VA US

Table 27: Virginia weather stations used in surface chloride concentration prediction

Region	NCDC Station Name
1	BACK BAY VIRGINIA VA
1	BACK BAY WILDLF REF VA US
1	'COLONIAL BEACH VA US'
1	'CORBIN VA US'
1	'EASTVILLE VA US'
1	'EMPORIA 1 WNW VA US'
1	'GREAT DISMAL NWR VIRGINIA VA US'
1	'HOLLAND 1 E VA US'
1	'HOPEWELL VA US'
1	'LANGLEY AIR FORCE BASE VA US'
1	'NEWPORT NEWS INTERNATIONAL AIRPORT VA US'
1	'NORFOLK INTERNATIONAL AIRPORT VA US'
1	'NORFOLK NAS VA US'
1	'OCEANA NAS VA US'
1	'PAINTER 2 W VA US'
1	'RICHMOND INTERNATIONAL AIRPORT VA US'
1	'STONY CREEK 2 N VA US'
1	'SUFFOLK LAKE KILBY VA US'
1	'TANGIER ISLAND VA US'
1	'WAKEFIELD 1 NW VA US'
1	'WAKEFIELD MUNICIPAL AIRPORT VA US'
1	'WALKERTON 2 NW VA US'
1	'WALLACETON LK DRUMND VA US'
1	'WALLOPS ISLAND WALLOPS FLIGHT FACILITY VA US'
1	'WARSAW 2 NW VA US'
1	'WEST POINT 2 NW VA US'
1	'WILLIAMSBURG 2 N VA US'
2	AMELIA 4 SW VA US
2	ASHLAND HANOVER CO MUNICIPAL AIRPORT VA US
2	ASHLAND VA US
2	BREMO BLUFF VA US'
2	'BUCKINGHAM VA US'
2	'CAMP PICKETT VA US'
2	'CHASE CITY VA US'
2	'CLARKSVILLE VA US'
2	'CROZIER VA US'
2	'FARMVILLE 2 N VA US'
2	'FREDERICKSBURG SEWAGE VA US'
2	'GORDONSVILLE 3 S VA US'
2	'JOHN H KERR DAM VA US'
2	'KEYSVILLE 2 S VA US'

2	'LAWRENCEVILLE 3 E VA US'
2	'LOUISA VA US'
2	'PALMYRA 3 S VA US'
2	'POWHATAN VA US'
2	'WINTERPOCK 4 W VA US'
3	APPOMATTOX VA US
3	BEDFORD VA US
3	'BROOKNEAL VA US'
3	'CHARLOTTE COURT HOUSE VA US'
3	'CHARLOTTESVILLE 2 W VA US'
3	'CHARLOTTESVILLE ALBEMARLE AIRPORT VA US'
3	'CHATHAM VA US'
3	'CONCORD 4 SSW VA US'
3	'DANVILLE REGIONAL AIRPORT VA US'
3	'DANVILLE VA US'
3	'FREE UNION VA US'
3	'HUDDLESTON 4 SW VA US'
3	'LYNCHBURG NUMBER 2 VA US'
3	'LYNCHBURG REGIONAL AIRPORT VA US'
3	'MARTINSVILLE FLT PLANT VA US'
3	'MEADOWS OF DAN 5 SW VA US'
3	'MONTICELLO VA US'
3	'PEDLAR DAM VA US'
3	'PHILPOTT DAM 2 VA US'
3	'ROCKY MOUNT VA US'
3	'SOUTH BOSTON VA US'
3	'STUART VA US'
3	'TYE RIVER 1 SE VA US'
3	'WOOLWINE 4 S VA US'
4	BIG MEADOWS VA US
4	BOSTON 4 SE VA US
4	'EDINBURG VA US'
4	'FORT VALLEY VIRGINIA VA US'
4	'FRONT ROYAL VA US'
4	'GORE 3 E VA US'
4	'LAKE OF THE WOODS VA US'
4	'LINCOLN VA US'
4	'LURAY 5 E VA US'
4	'MOUNT WEATHER VA US'
4	'PIEDMONT RESEARCH STATION VA US'
4	'QUANTICO MCAS VA US'
4	'SOMERSET VA US'
4	'SPERRYVILLE VA US'

4	'STAR TANNERY VA US'
4	'STERLING RCS VA US'
4	'THE PLAINS 2 NNE VA US'
4	'VIENNA VA US'
4	'WARRENTON 3 SE VA US'
4	'WASHINGTON DC DULLES INTERNATIONAL AIRPORT VA US'
4	'WASHINGTON REAGAN NATIONAL AIRPORT VA US'
4	'WINCHESTER 7 SE VA US'
4	'WINCHESTER VA US'
4	'WOODSTOCK 2 NE VA US'
5	'BUCHANAN VA US'
5	'BUENA VISTA VA US'
5	'COVINGTON FILTER PLANT VA US'
5	'CRAIG VALLEY VIRGINIA VA US'
5	'CRAIGSVILLE 2 S VA US'
5	'DALE ENTERPRISE VA US'
5	'EARLEHURST VA US'
5	'GATHRIGHT DAM VA US'
5	'GLASGOW 1 SE VA US'
5	'GOSHEN VA US'
5	'HOT SPRINGS VA US'
5	'KERRS CREEK 6 WNW VA US'
5	'LEXINGTON VA US'
5	'LIME KILN VIRGINIA VA US'
5	'MILLGAP 2 NNW VA US'
5	'MUSTOE 1 SW VA US'
5	'ROANOKE 8 N VA US'
5	'ROANOKE REGIONAL AIRPORT VA US'
5	'STAUNTON WATER TREATMENT PLANT VA US'
5	'UMHOLT VIRGINIA VA US'
5	'WAYNESBORO WATER TREATMENT VA US'
6	ABINGDON 3 S VA US
6	ALLISONIA 2 SSE VA US
6	BIG STONE GAP VA US
6	BLACKSBURG NATIONAL WEATHER SERVICE OFFICE VA US
6	BLAND VA US
6	BREAKS INTERSTATE PARK VA US
6	'BURKES GARDEN VA US'
6	'BYLLESBY 1 S VA US'
6	'CHRISTIANSBURG VA US'
6	'CLINTWOOD 1 W VA US'
6	'COPPER HILL VA US'
6	'FLOYD 2 NE VA US'

6	'GALAX RADIO WBRF VA US'
6	'GLEN LYN VA US'
6	'GRUNDY VA US'
6	'HILLSVILLE VA US'
6	'HURLEY 4 S VA US'
6	'JOHN FLANNAGAN LAKE VA US'
6	'LAFAYETTE 1 NE VA US'
6	'LEBANON VA US'
6	'NEWPORT 2 NNW VA US'
6	'NORTH FORK LAKE VA US'
6	'PAYNESVILLE 1 N VA US'
6	'PENNINGTON GAP VA US'
6	'PULASKI VA US'
6	'RICHLANDS VA US'
6	'SALTVILLE 1 N VA US'
6	'STAFFORDSVILLE 3 ENE VA US'
6	'TROUT DALE 3 SSE VA US'
6	'WILLIS VA US'
6	'WISE 3 E VA US'
6	'WISE VIRGINIA VA US'
6	'WYTHEVILLE VA US'